



OPEN ACCESS

EDITED BY

Pablo Grosse,
Consejo Nacional de Investigaciones
Científicas y Técnicas (CONICET),
Argentina

REVIEWED BY

Oswaldo González-Maurel,
University of Cape Town, South Africa
Axel Karl Schmitt,
Heidelberg University, Germany

*CORRESPONDENCE

Morgan J. Salisbury,
msalisbury@lowercolumbia.edu

SPECIALTY SECTION

This article was submitted to
Geochemistry,
a section of the journal
Frontiers in Earth Science

RECEIVED 11 April 2022

ACCEPTED 24 August 2022

PUBLISHED 03 October 2022

CITATION

Salisbury MJ, Jiménez N and Barfod D
(2022), $^{40}\text{Ar}/^{39}\text{Ar}$ ages and geochemistry
of the Intersalar Range of the Bolivian
Altiplano: A volcanological transect
spanning the arc and reararc of the
Central Andean Plateau.
Front. Earth Sci. 10:917488.
doi: 10.3389/feart.2022.917488

COPYRIGHT

© 2022 Salisbury, Jiménez and Barfod.
This is an open-access article
distributed under the terms of the
[Creative Commons Attribution License
\(CC BY\)](https://creativecommons.org/licenses/by/4.0/). The use, distribution or
reproduction in other forums is
permitted, provided the original
author(s) and the copyright owner(s) are
credited and that the original
publication in this journal is cited, in
accordance with accepted academic
practice. No use, distribution or
reproduction is permitted which does
not comply with these terms.

$^{40}\text{Ar}/^{39}\text{Ar}$ ages and geochemistry of the Intersalar Range of the Bolivian Altiplano: A volcanological transect spanning the arc and reararc of the Central Andean Plateau

Morgan J. Salisbury^{1*}, Néstor Jiménez² and Dan Barfod³

¹Department of Earth Sciences, Durham University, Durham, United Kingdom, ²Universidad Mayor de San Andrés, Instituto de Investigaciones Geológicas y del Medio Ambiente, La Paz, Bolivia, ³NEIF Argon Isotope Laboratory, SUERC, East Kilbride, United Kingdom

The volcanic Intersalar Range of western Bolivia provides a unique opportunity to examine geochemical variations spanning the arc and reararc regions of the Central Andean Plateau. In this study we report 23 new $^{40}\text{Ar}/^{39}\text{Ar}$ ages, 15 whole-rock Sr-Nd-Pb isotope analyses, and 50 whole-rock major and trace element analyses from samples collected across ~115 km of the Intersalar Range. Most samples are classified as trachyandesites and trachydacites, with the most mafic lavas (slightly alkaline, basaltic trachyandesites) erupting from the Pliocene Coracora volcano in the central Altiplano. We identify two distinct pulses of reararc magmatism: a Miocene phase between 20 Ma and 14 Ma that corresponds with local compressional shortening, and a Plio-Pleistocene phase between 5 and 1 Ma that postdates observed structural deformation in the region. $^{87}\text{Sr}/^{86}\text{Sr}$ values (0.70512–0.70600) and $^{143}\text{Nd}/^{144}\text{Nd}$ values (0.51226–0.51255) are generally higher, and lower, respectively, in the younger phase, whereas Pb isotopes ($^{206}\text{Pb}/^{204}\text{Pb} = 17.7315\text{--}18.5095$; $^{207}\text{Pb}/^{204}\text{Pb} = 15.5714\text{--}15.6279$; $^{208}\text{Pb}/^{204}\text{Pb} = 37.7862\text{--}38.6156$) show little variation with age. Isotope values are only loosely correlated with distance from the modern Central Volcanic Zone. Higher Sr/Y, Dy/Yb, and $[\text{La}/\text{Yb}]_N$ values in the Plio-Pleistocene samples are consistent with homogenization at the base of a thicker continental crust compared to the Miocene samples. Nb concentrations show the strongest correlation with distance into the reararc compared to all other trace elements (arc Nb = 6–16 ppm; reararc Nb = 12–26 ppm). Nb/Nb* values (a measurement of the depth of the negative Nb anomaly) correspondingly increase into the reararc (indicating smaller anomalies), reaching a maximum at Coracora volcano before decreasing in the far rear arc region. Compiled data across the Central Andean Plateau reveal a strong correlation between Nb/Nb* and the presence of intact mantle lithosphere beneath the central Altiplano. We interpret this distinct Nb signal to reflect melting triggered by the breakdown of Nb-rich hydrous minerals within foundering (delaminating) mantle lithosphere. In conjunction with spatiotemporal data, Nb systematics provide the clearest indication of mantle lithosphere in regions where mafic samples are not present.

KEYWORDS

Central Andes, volcanism, whole-rock and isotope geochemistry, $^{40}\text{Ar}/^{39}\text{Ar}$ age dating, Bolivia Altiplano

Introduction

The Central Andean Plateau, also known as the Altiplano-Puna Plateau, is the second largest crustal plateau on Earth and the only to coincide with active continental arc volcanism. Its enigmatic formation at a subduction boundary in the absence of continental collision has led numerous researchers to examine the complex temporal, structural, and magmatic history of the plateau (see Oncken et al., 2006; Trumbull et al., 2006; Barnes and Ehlers, 2009 for reviews). Despite numerous advances, the mantle sources, and their melting triggers, across much of the plateau remain poorly constrained, particularly in regions that lack mafic volcanism. A considerable factor limiting our knowledge of the intimate relationship between magmatism and orogeny in the Central Andes is an incomplete dataset of the ages and compositions of the abundant plateau volcanism. The rare mafic magmatism in the dominantly compressive Central Andes further complicates our understanding of petrogenesis in the region. In this context, radiometric ages of volcanism are an essential piece of the puzzle, as they provide unequivocal data revealing the time and location of melting events. In this study we evaluate spatial, temporal, and geochemical data of an arc-normal transect along the Intersalar Range of western Bolivia ($\sim 19.5\text{--}20.0^\circ\text{S}$, $\sim 67.5\text{--}68.7^\circ\text{W}$) and the broader plateau at this latitude to address the primary sources and melting triggers of the Central Andean Plateau at this latitude. Despite limitations, geochemical data of non-basaltic volcanism can provide significant insight, particularly when considered within a broader spatiotemporal framework.

The intersalar range

The Intersalar Range (*Serranía Intersalar* in Spanish on Bolivian geologic maps) is named after its location between two of the world's largest salt flats (Salar de Uyuni and Salar de Coipasa) on the Bolivian Altiplano. The Intersalar Range is a series of composite volcanic centers, flat lava domes known as tortas, and extensive ignimbrites that extend eastward from the Western Cordillera into the central Altiplano of Bolivia (Figures 1–3). The western portion of the Intersalar Range blends into the north-south trending Central Volcanic Zone (CVZ) arc along the Bolivia/Chile border. The eastern extent of the range is loosely defined by the composite centers of Coracora and Tunupa, with volcanism extending further east in the form of structurally aligned monogenetic magmatism of the central and eastern Altiplano (Davidson and de Silva, 1992, 1995), and the immense Los Frailes volcanic complex (Jiménez and López-

Velásquez, 2008) near the fold and thrust belt of the Eastern Cordillera (Figure 1). This arc-perpendicular trend of volcanism coincides with the axis of topographic symmetry dividing the northern and southern portions of the Bolivian Orocline, and also marks the widest extent of the Central Andean Plateau (Allmendinger et al., 2005). In total, this arc-normal volcanic transect is among the most extensive of the entire plateau and coincides with one of its better structurally constrained sections (e.g., Beck and Zandt, 2002; Yuan et al., 2002; McQuarrie et al., 2005), thus allowing a detailed examination of the relationship between magmatism, plateau geometry, and structural deformation.

Prior to a geochemical and temporal analysis of lavas from Tunupa volcano (Salisbury et al., 2015), only limited geochemical and age information was available for the Intersalar Range. This range was mapped by Leytón and Jurado (1995) (Salinas de Garci Mendoza quadrangle, 1:250,000 scale) as consisting primarily of Miocene to Pleistocene lavas overlying extensive and gently folded pyroclastic deposits that crop out in both the eastern and western portions of the range (Figure 3). A potential collapse caldera was mapped by Leytón and Jurado (1995) near Cerro Mokho, however detailed analysis of ignimbrite stratigraphy and related structures will be necessary to confirm this hypothesis. Age estimates of Leytón and Jurado (1995) were based primarily on 12 dispersed K/Ar ages ranging from 17.6 ± 0.2 Ma to 1.8 ± 0.2 Ma and the relative amounts of erosion experienced by the volcanic centres. Hoke and Lamb (2007) added one geochemical analysis and a K/Ar age (2.57 ± 0.45 Ma) within the confines of the Intersalar Range as defined in the present study.

The results from Tunupa volcano demonstrated significant geochemical differences from volcanoes of the CVZ arc, and served as the impetus for the current study, which aims to use age-constrained geochemical data collected across the Intersalar Range and the broader plateau to evaluate various proposed reararc melting mechanisms and mantle sources. In the present study, we provide a strategic reconnaissance of $^{40}\text{Ar}/^{39}\text{Ar}$ ages, Sr-Nd-Pb isotope data, and whole-rock geochemical analyses of the Intersalar Range of western Bolivia. We then consider this dataset within the broader context of regional magmatism and the lithospheric geometry of the Central Andean Plateau revealed by geophysical data.

Geologic setting

The Intersalar Range is oriented orthogonally to both the Peru-Chile trench and the main trend of the CVZ arc of the Western Cordillera, extending ~ 120 km from the Chile/Bolivia border into the center of the internally drained Altiplano basin in

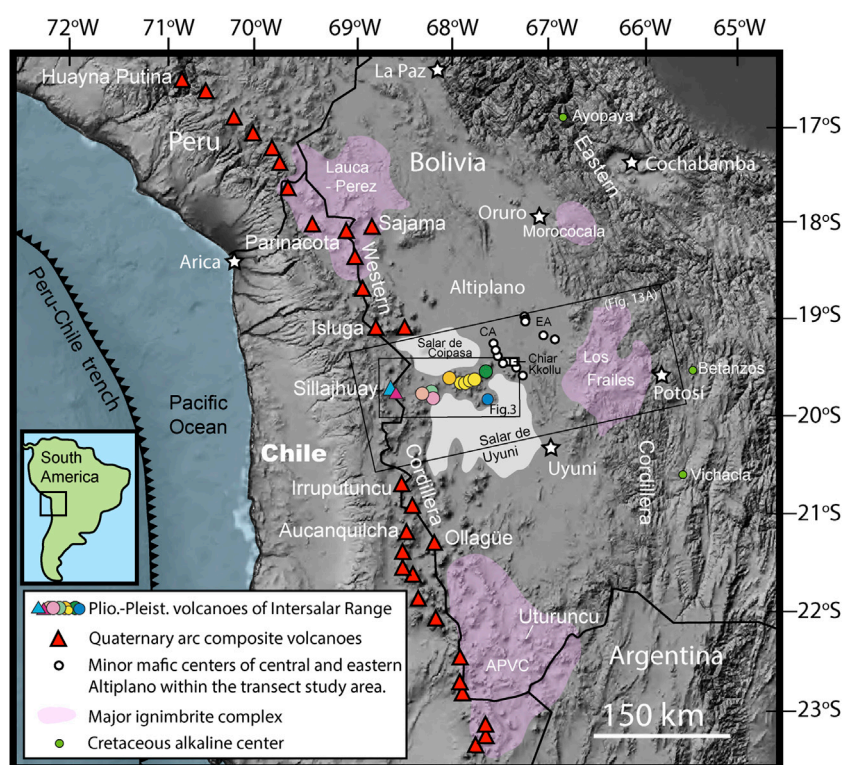


FIGURE 1
 Location of the Intersalar Range volcanoes (colored symbols) of the Bolivian Central Andean Plateau in South America. Symbols are consistent in all subsequent figures. The labeled minor mafic centers of the central Altiplano (CA), eastern Altiplano (EA), and the Cretaceous-rifting related alkaline rocks of Ayopaya, Betanzos, and Vichacla are discussed in the text and included in subsequent figures for comparison with the data of this study. Not all volcanic centers in the map region are labeled in this figure. References in subsequent figures and text. Shaded relief digital elevation model (DEM) background image derived from 90 m resolution SRTM data.

Bolivia (Figure 1). The immense Central Andean Plateau is an elevated region between 14°S and 28°S, defined by a contour greater than 3,000 m. a.s.l. With individual peaks approaching 7,000 m. a.s.l. (Barnes and Ehlers, 2009). The plateau is morphologically divided at ~22°S into the northern Altiplano and the southern Puna regions, and from west to east into the Precordillera, Western Cordillera, Altiplano/Puna basins, Eastern Cordillera, Interandean zone, and the Subandean Range. The Quaternary CVZ arc is located along the Western Cordillera and spans nearly the entire extent of the plateau from 14°S to 27°S. In the latitude of the Intersalar Range, Wörner et al. (1992) recognized a relative lack of Quaternary composite volcanism in the Alto de Pica region between Isluga and Irruputuncu volcanoes, which coincides with a change in Pb isotopic compositions that are interpreted to reflect interaction of magmas with domains of different crustal type and age. Although later investigation would identify Quaternary complexes in both Chile (Polanco and Gardeweg, 2000; Correa, 2011) and Bolivia (this study), this segment of the arc, known as the “Pica Gap” is notable for an apparent lack of Late Pleistocene to Holocene volcanism, and for a lack of tectonic horsts, which are typical for

the entire CVZ both to the north and south (Wörner et al., 1994). See Gardeweg and Sellés (2017) for a discussion of the Pica Gap in northern Chile.

The continental crust of the Central Andes is among the thickest in the world (up to 80 km) and Moho depths vary significantly throughout the plateau (Yuan et al., 2002; McGlashan et al., 2008). At the latitude of the Intersalar Range (~19–20°S), the Western Cordillera and Eastern Cordillera are underlain by ~70 km, and ~80 km-thick-crust, respectively, although the crust only reaches to depths of ~57 km beneath the eastern portion of the Intersalar Range in the central Altiplano (Yuan et al., 2002). The geophysical data further suggest that this crust is dominantly felsic with very little, if any, mafic component (Beck and Zandt, 2002; Yuan et al., 2002). Lithospheric thickness variations follow an inverted pattern compared to the crust at 19–20°S: Beck and Zandt (2002) identified a root of mantle lithosphere that extends to depths of ~150 km beneath the central Altiplano, but is essentially absent beneath both the Western and Eastern Cordilleras. These values are in stark contrast to the ~200 km thick lithosphere of the Brazilian craton and are interpreted to

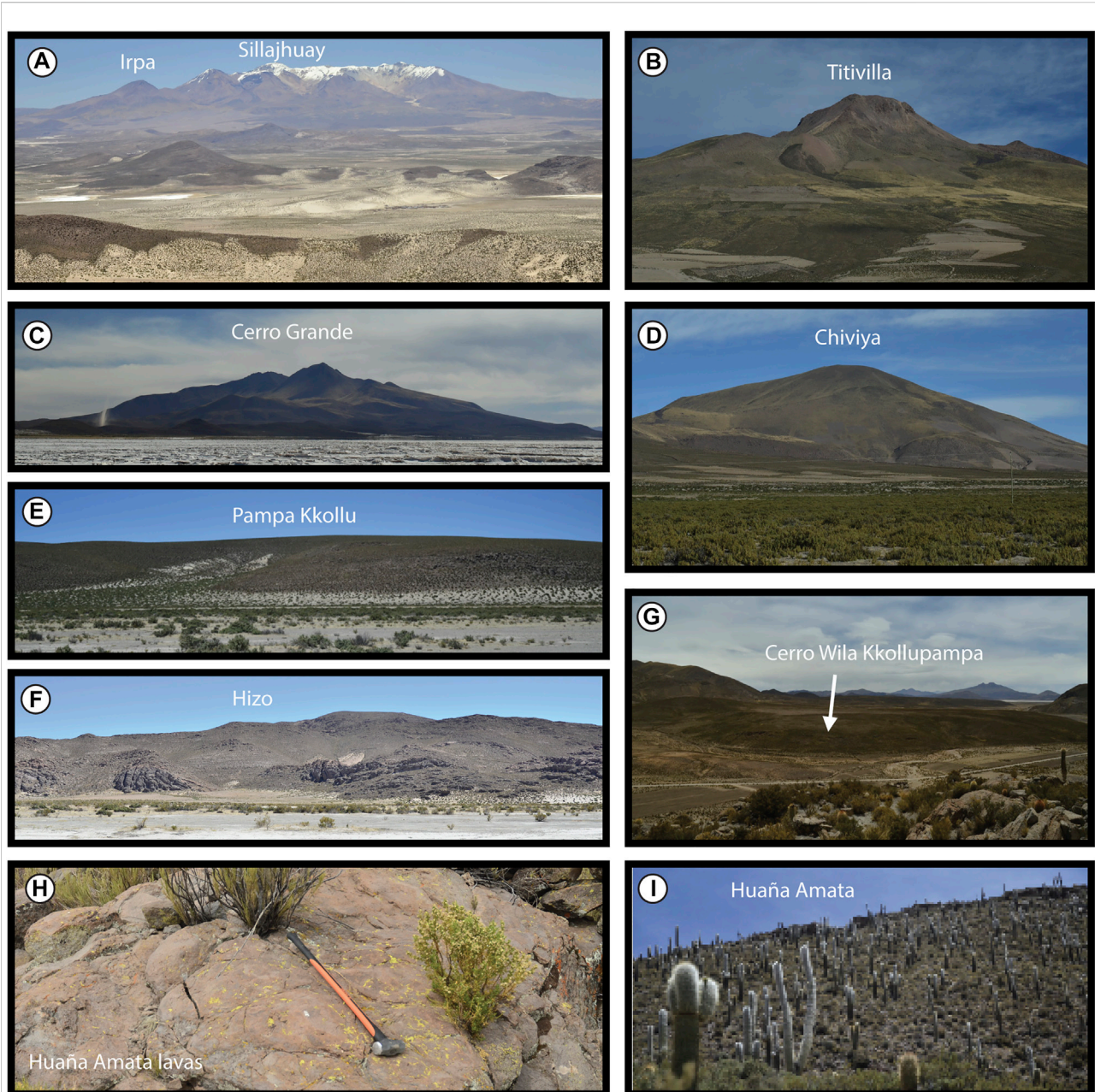


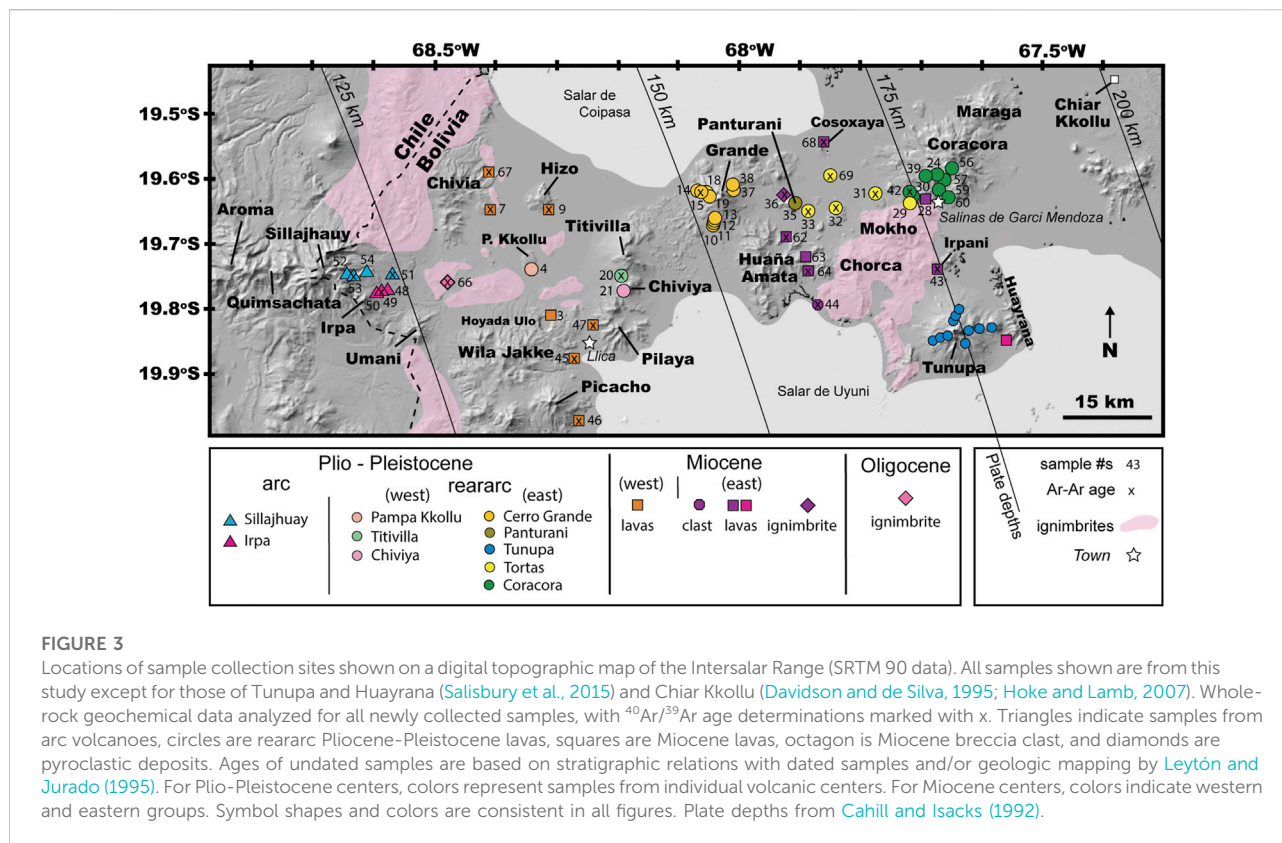
FIGURE 2

Field photographs showing examples of Intersalar Range volcanism. (A) View towards the arc composite centers of Sillajhuay and Irpa volcanoes along the Bolivia/Chile Border, image taken from Chiviya volcano. (B–D) Rear arc composite centers Titivilla, Grande, and Chiviya. (E–F) Smaller silicic centers in the western Intersalar Range: Pampa Kkollu and a previously unnamed center near estancia Hizo. (G) Cerro Wila Kkollupampa, one of the five, broad, flat-topped, relatively mafic tortas sampled in the eastern Intersalar Range. (H–I) Miocene Huaña Amata volcanic center showing typical examples of weathering and vegetation of the Intersalar Range.

result from piecemeal foundering (delamination) of the mantle lithosphere and mafic lower crust (Beck and Zandt, 2002).

Although few exposed structures exist within the Intersalar Range, our data can be interpreted within the framework of deformation recorded by nearby structures and related sedimentation. Southwest of the study area in the western

flank of the Western Cordillera and Precordillera (20–21°S, 69°W), deformation is interpreted to have occurred in two stages, the first between ~45 and ~37 Ma, and the second between ~17 and ~10 Ma (Victor et al., 2004). This second stage of deformation is largely coincident with shortening related to the Yazón Anticline (20.4°S, 67.9°W) between



~21 and ~11 Ma with maximum rates at ~15 Ma, whereas structures exposed in the region of Uyuni indicate shortening between ~35 and 10 Ma in the eastern Altiplano (Elger et al., 2005). Also in the eastern Altiplano, ~30 km east of the Intersalar Range, the numerous reverse faults and folds of Tambo Tambillo (19–20°S, 68°W) indicate shortening in the central Altiplano between ~14 and ~5 Ma, which largely overlaps with ~14 to ~9 Ma deformation of the Corque syncline ~160 km to the north (Kennen et al., 1995). As the observed structural deformation of the Altiplano is apparently insufficient to account for its extreme crustal thickness, ductile flow of hot, lower crust from the Eastern Cordillera may have contributed up to 40% of the Altiplano crust (Husson and Sempere, 2003).

Proposed petrogenetic models of Bolivian Altiplano volcanism

Cenozoic reararc magmatism of Bolivia has long been of interest to Andean researchers as the large distances from the CVZ arc suggest an intriguing relationship between the construction of the Central Andean Plateau and reararc magmatism. However, the primary melting triggers and the relative contributions of mantle asthenosphere, mantle lithosphere, and continental crust in the genesis of plateau

magmas remain difficult to constrain (e.g., Hildreth and Moorbath, 1988; Rogers and Hawkesworth, 1989; Davison and de Silva, 1992; Davison and de Silva, 1995; Hoke and Lamb, 2007; Jiménez and López-Velásquez, 2008; Salisbury et al., 2015). In a study of 15 volumetrically minor, monogenetic lavas of the central and eastern Altiplano (Figure 1), Davidson and de Silva (1995) favored a petrogenetic model where low degrees of partial melting of the asthenosphere is triggered by dehydration of the Nazca plate in the far reararc region, where these melts are then subject to significant geochemical modification at the base of the thick continental crust. Hoke and Lamb (2007) took advantage of a more comprehensive dataset and significant advances in geophysical measurements of the region and argued that magmatism of the Bolivian Altiplano was strongly influenced by a widespread lithospheric removal event in the Late Oligocene/Early Miocene that created irregular depths of the mantle lithosphere and allowed long-term decompression melting of the asthenosphere beneath the Los Frailes volcanic complex and lateral melt migration to centers beneath the central Altiplano and the eastern Intersalar Range. In contrast, Salisbury et al. (2015) proposed that the high Nb concentrations in the Pleistocene lavas from Tunupa volcano more likely signaled a strong influence of melted hydrated mantle lithosphere, triggered by localized piecemeal foundering. Each of these models are evaluated below in the Discussion section.

Sample collection and analytical methods

Field collection

Sampling of the Bolivian Intersalar Range was carried out during three field campaigns to the western Altiplano in 2012 (Figure 3). In total, 72 samples were collected with 50 samples later selected for detailed chemical analyses, which are reported in this study. Of the 50 new analyses, 47 are from effusive lava flows, 2 are from explosive eruptions, and one is from an intrusive stock collected from Coracora volcano. Ignimbrite matrix (sample #66) was collected ~23 km east of the summit of Sillajhuay, near Rio Cancosa, from a widespread, and apparently large-volume, ignimbrite of the western Altiplano. Pumice (sample #36) was extracted from a small-volume, and apparently locally sourced, ignimbrite on the northwest flank of Panturani. The 47 samples of lava were collected from 22 individual centers from both the arc and reararc regions, spanning ~115 km. Multiple samples were collected from morphologically distinct lava flows from the composite centers of Sillajhuay, Irpa, Chivia, Grande, Huaña Amata and Coracora, whereas only single samples were collected from the composite centers of Wila Jakke, Hoyada Ulo, Picacho, Pilaya, Titivilla, Chiviya, and Panturani. Single samples were also collected from the flat-topped, apparently monogenetic tortas of Wila Kkollupampa, Tenica Loma, Jachcha Pallallí, Uta Kkollu, and Tuju Tujuni that erupted between Grande and Coracora, as well as the smaller, relatively isolated centers of Hizo, Pampa Kkollu, Cosoxaya, and Irpani. The lavas of Cosoxaya and Irpani were not mapped by Leytón and Jurado (1995) and are named here based on local landmarks. The Hizo center is enigmatic as there are apparent flow structures reminiscent of a vent location of large-volume ignimbrites (e.g., Salisbury et al., 2011), however, detailed field and laboratory investigation is necessary to better understand this center. A dark, angular clast (sample #44) was removed from a sedimentary breccia containing a homogenous load of 15–30 cm cobbles on the northern shore of Salar de Uyuni south of Huaña Amata. As chemical alteration is common in the Intersalar Range, care was taken to find the least-altered samples in the field and to remove weathering rinds when necessary. Appropriate samples for age and geochemical analyses were selected following thin-section analysis.

$^{40}\text{Ar}/^{39}\text{Ar}$ geochronology

In total, 23 samples representing 21 different volcanic centers were selected to provide a comprehensive overview of the age of Intersalar Range volcanism. Petrographic analysis was used to identify potassium-bearing phases and to select suitable samples with low degrees of alteration for $^{40}\text{Ar}/^{39}\text{Ar}$ dating.

Sanidine was prioritized, although only available for analysis in four samples. Plagioclase phenocrysts were selected for nine samples, and unaltered, phenocryst-free groundmass consisting of glass and plagioclase microlites were chosen for the 10 samples without suitable potassium-bearing phenocrysts. Eighteen samples (groundmass or feldspar) were run as step-heating experiments and presented in plateau and inverse isochron diagrams. Seven samples of feldspar were run as sets of single grain total-fusion experiments and presented as probability density function plots. Two of these (#66, 68) were analyzed by both methods. Samples and neutron flux monitors were stacked in quartz tubes with the relative positions of packets precisely measured for later reconstruction of neutron flux gradients. The sample package was irradiated in the Oregon State University reactor, Cd-shielded facility. Alder Creek sanidine (1.1891 ± 0.0008 , Ma, 1σ , Niespolo et al., 2017) was used to monitor ^{39}Ar production and establish neutron flux values (J) for the samples.

$^{40}\text{Ar}/^{39}\text{Ar}$ data were collected at the Scottish Universities Environmental Research Centre (SUERC) NERC Argon Isotope Facility (East Kilbride) on a GVi instruments ARGUS V multi-collector mass spectrometer using a variable sensitivity Faraday collector array in static collection (non-peak hopping) mode (Sparks et al., 2008; Mark et al., 2009) for step heating, and an MAP-215–50 single-collector instrument equipped with an electron multiplier for single grain analyses. Gas was extracted from samples via step-heating using a mid-infrared (10.6 μm) CO_2 laser with a non-gaussian, uniform energy profile and a variable beam diameter. The samples were loaded into a copper planchette, housed in a doubly-pumped ZnS-window laser cell, evacuated to UHV conditions. Liberated argon was purified of active gases (e.g., CO_2 , H_2O , H_2 , N_2 , CH_4) using three Zr-Al getters; one at 16°C and two at 400°C . Time-intensity data were regressed to t_0 with second-order polynomial fits to the data. The average total system blank ($\pm 2\sigma$) for laser extractions, measured between each sample run over the temperature range where age information is extracted, was $8.9 \pm 6.4 \times 10^{-16}$ mol ^{40}Ar , $1.1 \pm 2.3 \times 10^{-16}$ mol ^{39}Ar , $2.7 \pm 3.8 \times 10^{-17}$ mol ^{36}Ar (ARGUS) and $1.2 \pm 0.8 \times 10^{-15}$ mol ^{40}Ar , $0.8 \pm 4.6 \times 10^{-17}$ mol ^{39}Ar , $1.2 \pm 0.3 \times 10^{-17}$ mol ^{36}Ar (MAP). Mass discrimination was monitored daily, between sample runs by analysis of an air standard aliquot delivered by an automated pipette system over the course of the 2-month analysis period. ARGUS: for $n=306$ air standards the mass fractionation factor (D) was determined to be 0.9994 ± 0.0019 . MAP: for $n=314$ air standards the mass fractionation factor (D) was determined to be 1.0109 ± 0.0029 . See raw data in [Supplementary Material](#) for D values applied to individual steps.

Plateau ages were identified by the following criteria: (1) Steps overlap in age within 2σ uncertainty; (2) a minimum ^{39}Ar content for a step is $\geq 0.1\%$ of total ^{39}Ar release; (3) the plateau consists of at least five contiguous steps; (4) a minimum of 50% of ^{39}Ar in the chosen steps; (5) the inverse isochron formed by the plateau steps yields an age indistinguishable from the plateau age

at 2σ uncertainty; (6) the trapped component composition, derived from the inverse isochron, is indistinguishable from the composition of air at the 2σ uncertainty level; (7) age and uncertainty (SEM) were calculated using the mean weighted by the inverse variance of each step; (8) for replicated samples, a plateau for each aliquot was independently calculated and the accepted steps for each aliquot combined into a composite isochron and composite plateau; and (9) the dispersion of data points, as indicated by MSWD, on the isochron and plateau diagrams are comparable to the expected analytical scatter for a given number of steps (Wendt and Carl 1991).

Peak age distributions in probability density function plots were defined by determining the best contiguous group of individual grain analyses that conforms to a Gaussian distribution with the expected scatter as indicated by the value of MSWD (Wendt and Carl 1991). Grains with large age uncertainties of $>100\%$ or low radiogenic yields of $<20\%$ $^{40}\text{Ar}^*$ were rejected prior to calculating the probability distributions. All blank, interference, and mass discrimination calculations were performed with the *MassSpec* software package version 8.058 (Deino, 2015). Plateau ages, or composite plateau ages for replicated samples, were chosen as the best estimates of the emplacement ages. Ages are reported with 2σ analytical uncertainties.

Whole-rock analyses

50 new analyses of whole-rock major- and trace-elements were performed at the Geo-Analytical Laboratory at Washington State University–Pullman under the direction of Richard Conrey, Lauren Wagoner, and Charles Knaack in 2013. Whole-rock major-element concentrations were analyzed by X-ray fluorescence (XRF) using lithium tetraborate fused beads and a Rigaku 3,370 spectrometer with a Rh target. Trace-element concentrations were measured by XRF and inductively coupled plasma–mass spectrometry (ICP-MS). Repeat analysis of standard GSP-2 over the analysis period suggests long term precision and accuracy of $<2\%$ for all major elements analyzed by XRF, except FeO^* where accuracy is $<3\%$. For trace elements analyzed by XRF precision and accuracy is $<10\%$ for all elements except for Sc ($<16\%$), and U ($<70\%$). Repeat analysis of samples by ICP-MS show precision $<1\%$ – 5% for all elements analyzed. In cases where the same element was measured by both methods, such as Sc and U, ICP-MS results are reported. See Johnson et al. (1999) and Knaack et al. (1994) for detailed analytical methodology. The whole-rock major and trace element data collected by Salisbury et al. (2015) used the same laboratory and methods as the present study and are included in the figures of this study. The Tunupa study provides context on the range of data expected at individual composite centers.

Fourteen of the samples dated by $^{40}\text{Ar}/^{39}\text{Ar}$, and one undated sample of presumed Pleistocene age, were analyzed

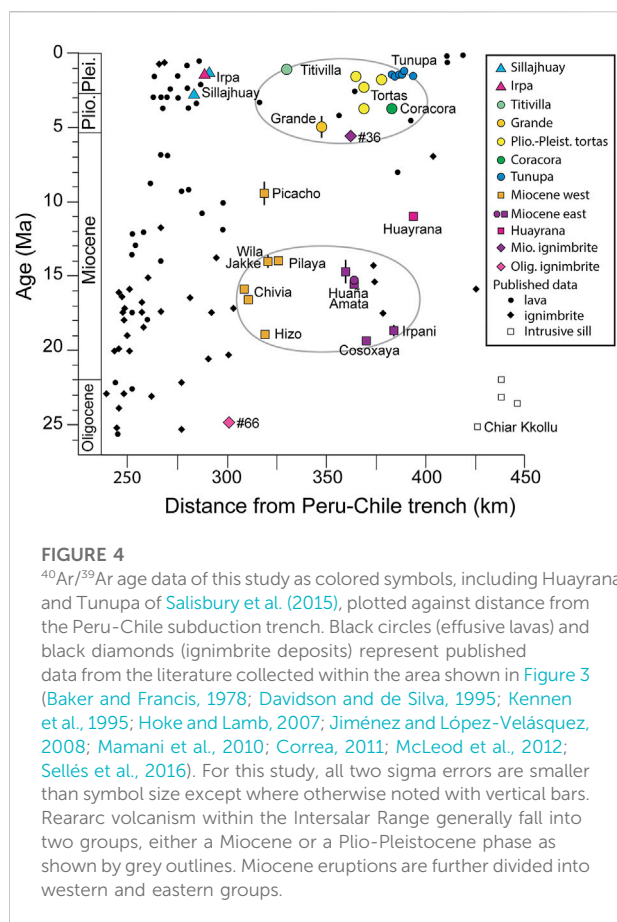
for Sr, Nd, and Pb isotopes using a ThermoElectron Neptune multi-collector ICP-MS system at the Arthur Holmes Isotope Geochemistry Laboratory at the University of Durham in 2014 under the guidance of Dr. Geoff Nowell. Details of the operating procedures and instrument configuration are described in detail in Handley et al. (2007) and references therein. Data quality was monitored by frequent analysis of standard reference materials throughout each analytical session. Measurement of isotope standards returned the following values: NBS-987 $^{87}\text{Sr}/^{86}\text{Sr} = 0.710264 \pm 0.000016$ (2s) ($n = 16$); J&M Nd isotope standard 0.511106 ± 0.00012 (2s) ($n=15$); and NBS-981 $^{206}\text{Pb}/^{204}\text{Pb} = 16.9415 \pm 0.0011$ (2s), $^{207}\text{Pb}/^{204}\text{Pb} = 15.4987 \pm 0.0011$ (2s), $^{208}\text{Pb}/^{204}\text{Pb} = 36.7258 \pm 0.0037$ (2s), $^{207}\text{Pb}/^{206}\text{Pb} = 0.94185 \pm 0.00003$, $^{208}\text{Pb}/^{206}\text{Pb} = 2.16742 \pm 0.00012$ (2s) ($n=8$).

Results

$^{40}\text{Ar}/^{39}\text{Ar}$ age determinations

The twenty-three new $^{40}\text{Ar}/^{39}\text{Ar}$ ages presented here (Supplementary Table S1) range from Late Oligocene to Pleistocene (Figure 4). Plateau age spectra criteria were met for seventeen samples (ten groundmass, four plagioclase, and three sanidine). Probability density function ages are preferred for six samples. A high level of precision ($2\sigma < 1.4\%$ of age) was achieved for 14 of the plateau ages including those from sanidine, plagioclase, and groundmass, whereas a lower level of precision ($2\sigma = 1.5\%$ – 14% of age) is reported for three of the plagioclase plateau ages and the six probability ages (Supplementary Table S1; Figure 5). Most of the newly reported ages can be grouped into either an Early to Mid-Miocene phase between ~ 19.4 Ma and 14.0 Ma, or a Pliocene to Pleistocene phase between ~ 5 Ma and 1 Ma. The exceptions to these groups in the Intersalar Range are lavas from the silicic center of Picacho (9.49 ± 0.77 Ma), the ~ 8 Ma stock of Cerro Mokho (Leytón and Jurado, 1995), and the ~ 11 Ma lavas of Huayrana (Salisbury et al., 2015). The Miocene lavas are further divided into western and eastern groups (Figure 3 and subsequent figures).

The oldest dated sample of this study is from the ignimbrite matrix (sample #66) collected near Rio Cancosa on the western Altiplano. As suitable clasts of pumice could not be extracted, we acquired single-crystal fusion data for this sample that show an age peak of 24.87 ± 0.39 Ma. Three slightly older grains were rejected in this treatment, suggesting the presence of a minor population of foreign crystals in the ignimbrite and that the plateau age may be slightly biased toward an older age. We take the younger probability density function age as the best estimate of the timing of emplacement. If this age is reliable, it represents one of the oldest known eruptions at this latitude of western Bolivia and may correlate with ignimbrites in Chile of similar age (Sellés et al., 2016). We report an age of 15.626 ± 0.021 Ma for the



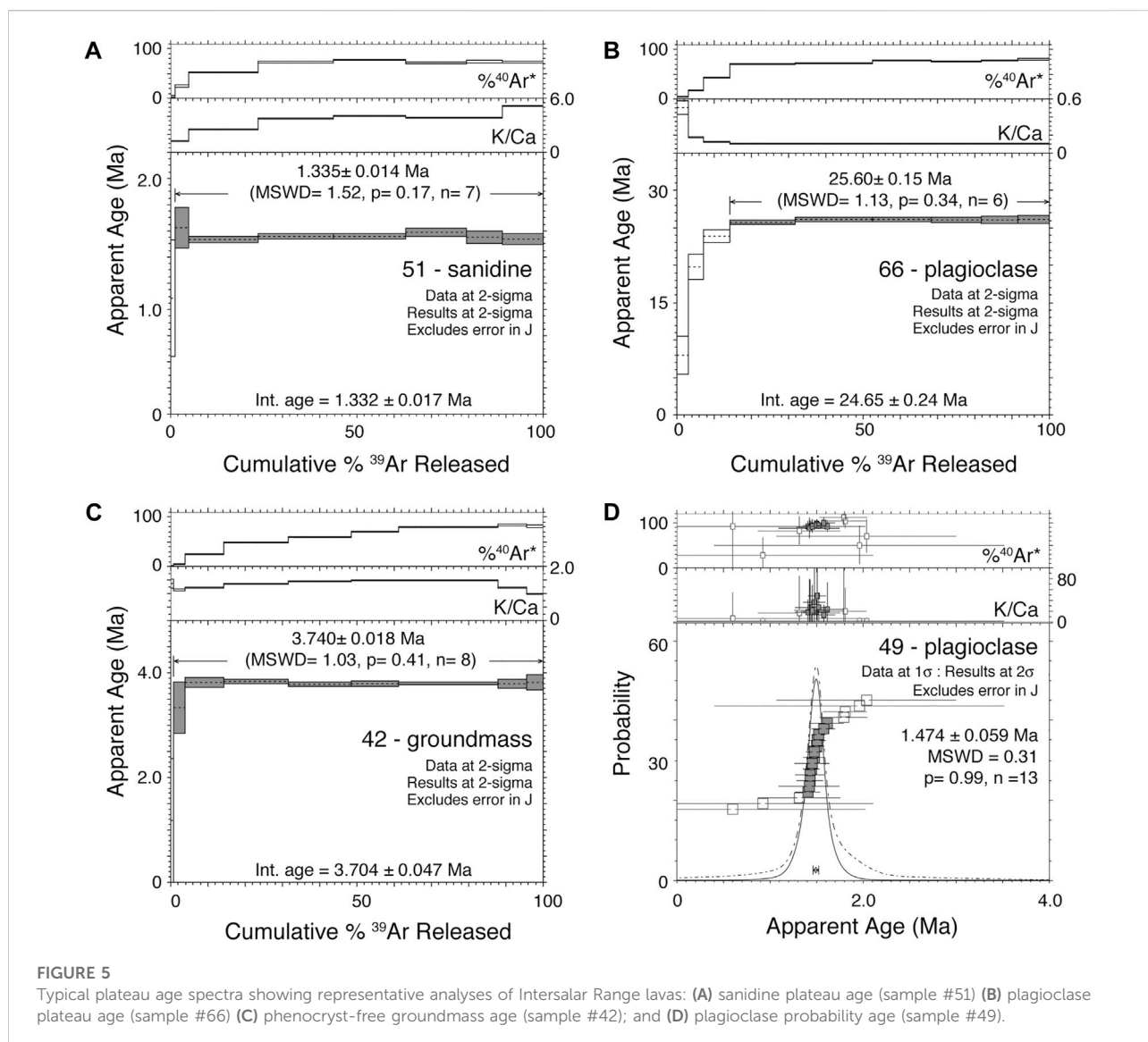
breccia clast collected south of the Oligocene to Miocene ignimbrite field of Cerro Chorca. Because of the homogeneity of the deposit, the angular clasts suggesting limited transportation, and similar ages (14.72 ± 0.79 and 15.31 ± 0.11 Ma) reported for two lavas collected from the nearby Huaña Amata center, this breccia clast is considered to be derived from a local source, most likely Huaña Amata.

Lavas from Titivilla volcano gave the youngest $^{40}\text{Ar}/^{39}\text{Ar}$ age (1.19 ± 0.11 Ma), although we note that the error for this plagioclase plateau age is higher than most of the other ages of this study. The four dated samples from the apparently low viscosity tortas between Grande and Coracora range between 3.785 ± 0.018 Ma (Jachcha Pallalli) and 1.611 ± 0.022 Ma (Uta Kkollu). The Jachcha Pallalli lavas (3.740 ± 0.018 Ma) are similar in age, morphology, and petrography to the lavas from the western flank of Coracora (sample #42), suggesting that these lavas may be related to the same eruptive episode. For the CVZ arc, our two sanidine plateau ages for Sillajhuay lava flows separated by 500 m of elevation indicate effusive volcanism on the eastern flanks of this large composite volcano at 2.7147 ± 0.0068 Ma and 1.335 ± 0.014 Ma. A plagioclase probability age of 1.457 ± 0.045 Ma for lavas from Irpa further suggest abundant arc activity at these centers in the Late Pliocene and Pleistocene.

Our age results are generally consistent with the relative age estimates of Leytón and Jurado (1995), with some noticeable exceptions: the lavas of Hizo were mapped as Pliocene or younger but gave a sanidine age of 18.877 ± 0.016 Ma; and samples from Sillajhuay and Titivilla gave Pleistocene ages, although they were mapped as Miocene-Pliocene. The Pleistocene Tunupa volcano was also mapped as Miocene-Pliocene although ages from seven individual eruptions indicate a Pleistocene history (1.6–1.2 Ma) for this edifice (Salisbury et al., 2015). We note that although the Salinas de Garci Mendoza quadrangle of Leytón and Jurado (1995) uses a Pliocene/Pleistocene boundary of 1.6 Ma, the $^{40}\text{Ar}/^{39}\text{Ar}$ ages mentioned above would still classify as Pleistocene under this scheme. Additionally, the tortas west of Coracora were mapped as Pleistocene to Holocene (younger than 1.6 Ma), although our age results from four of these tortas range from 3.84 to 1.63 Ma. The discrepancy between age estimates based on erosion and our new $^{40}\text{Ar}/^{39}\text{Ar}$ ages underscores the importance of precise radiometric age dating in the arid Central Andes. We use the boundary of 2.58 Ma for the Pliocene/Pleistocene throughout this manuscript.

Petrographic overview

Textures of Pliocene to Pleistocene Intersalar Range lavas generally fall into two categories (Supplementary Table S2; Figure 6) that correlate with the composition and type of volcanic center from which they erupted. Lavas from the more silicic (wt% $\text{SiO}_2 = \sim 60\%–65\%$) composite centers from both the main arc trend and the reararc region tend to be porphyritic (20%–35% phenocrysts) and are dominated by phenocrysts ($\sim 2–7$ mm) of plagioclase, or sanidine (Figure 6A). These lavas also contain abundant phenocrysts of biotite (5%–7%) and amphibole (4%–9%) with lesser amounts ($\leq 1\%$) of orthopyroxene and clinopyroxene. Embayed quartz xenocrysts with pyroxene reaction coronas are present in some samples as are glomerocrysts with the same phenocryst assemblages as the host lavas. The groundmass is dominated by abundant plagioclase microphenocrysts and microlites, often with a hyalopilitic texture. Apatite is a common accessory mineral in all samples. The more mafic (wt% $\text{SiO}_2 = \sim 57\%–59\%$) lavas associated with the smaller, monogenetic tortas are generally phenocryst poor (<5%–17%) and contain olivine (3%–5%, $\sim 0.2–1.0$ mm) as the primary phenocryst phase with lesser amounts of orthopyroxene, clinopyroxene, and partially to completely opacitized amphibole and biotite (Figures 6B,C). Partially resorbed quartz xenocrysts with pyroxene reaction coronas are also common in these samples. Glomerocrysts are common and are comprised dominantly of olivine. Groundmass textures are strongly hyalopilitic with abundant aligned microlites of plagioclase with some samples also containing microlites of olivine and pyroxene. Miocene lavas show petrographic diversity, although most are porphyritic with



abundant phenocrysts of plagioclase (10%–20%) and pyroxenes (2%–13%). The more mafic samples from Chivia located near the modern CVZ arc also contain olivine phenocrysts, whereas the Cosoxaya lavas from the eastern Intersalar Range contain a significant amount of amphibole (~6%) and biotite (~2%) phenocrysts. Mafic minerals from the Late Oligocene ignimbrite sample near Rio Cancosa were too altered for identification.

Whole-rock geochemistry

The volcanic rocks analyzed in this study (Supplementary Material) range from 53.7 to 76.4 wt% SiO₂ with most samples classified as trachyandesites to trachydacites on a total alkalis-

silica (TAS) diagram (Le Maitre et al., 1989) (Figure 7A). The most mafic samples of this study are basaltic trachyandesites collected from the Pliocene Coracora volcano, basaltic andesites from the Miocene Chivia lavas, and the trachyandesites of the Pliocene monogenetic tortas. Consistent with morphology indicating higher viscosity flows, the lavas of the composite centers are mostly trachyandesites to trachydacites. The most silicic samples are rhyolitic. Most Intersalar Range samples plot as subalkaline, with the more mafic Coracora lavas and nearby tortas plotting slightly alkaline (Irvine and Baragar, 1971). On a SiO₂ vs K₂O diagram, Intersalar Range samples plot almost entirely as high-K, calc-alkaline, with only a few of the most silicic samples plotting as shoshonitic (Figure 7B). On Harker diagrams with samples examined as a single suite, MgO, CaO, Al₂O₃, FeO, and TiO₂ are negatively correlated with silica

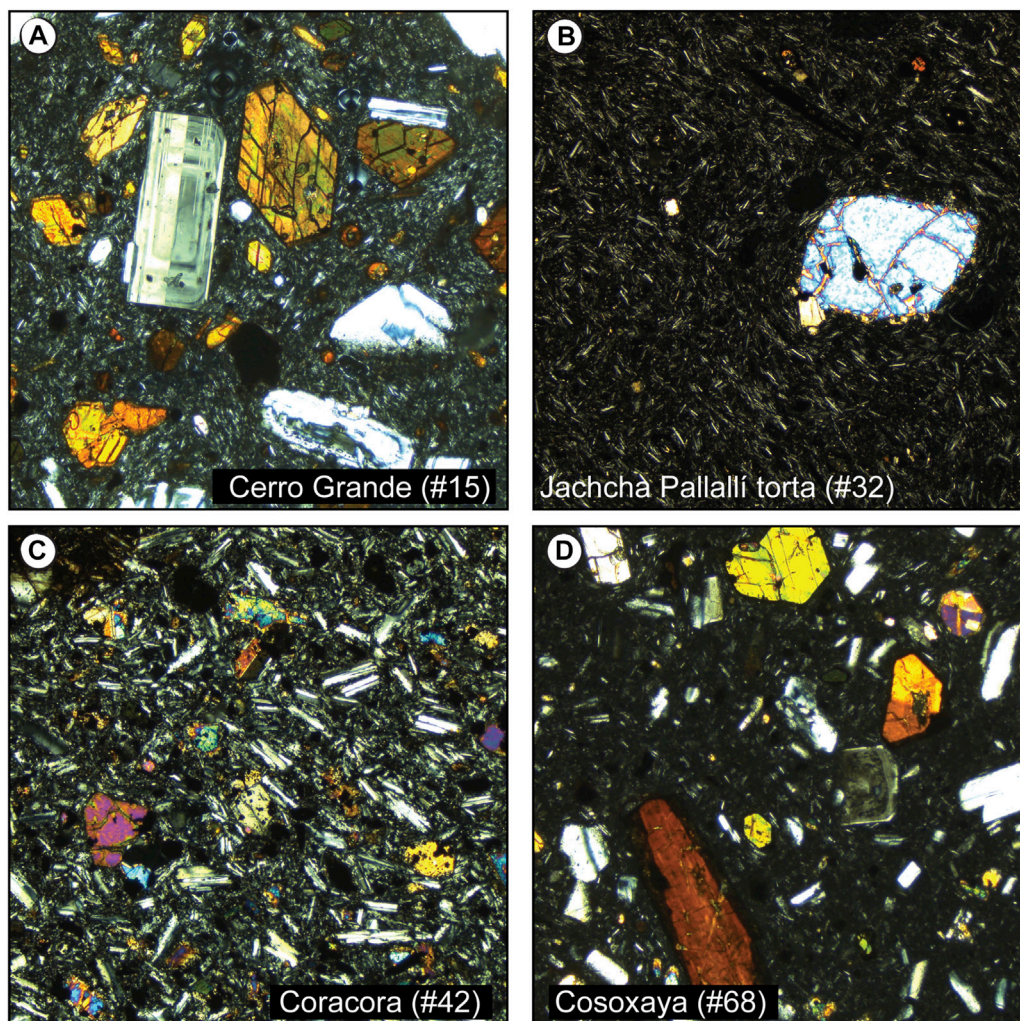


FIGURE 6

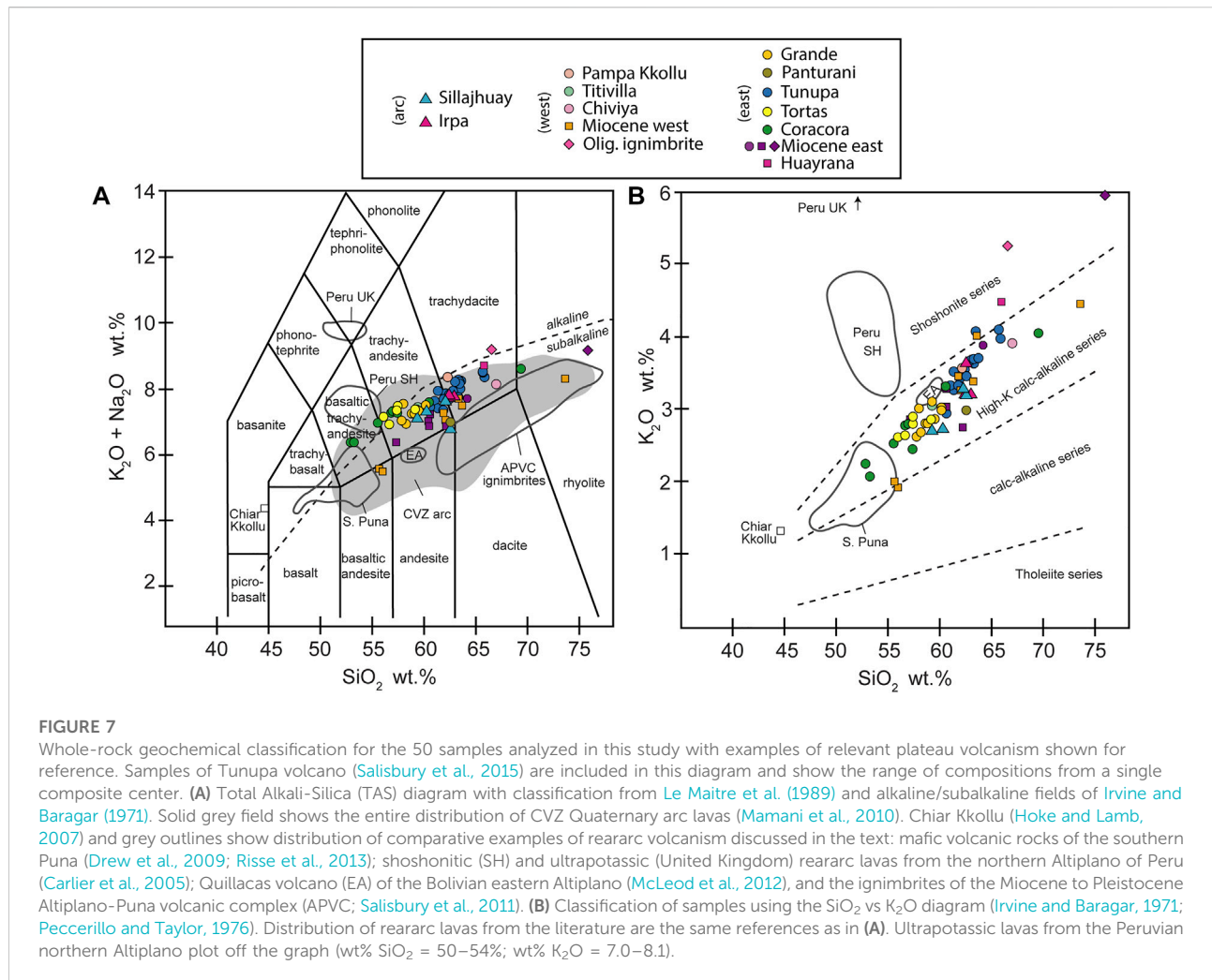
Photomicrographs in cross-polarized light of representative petrographic features of Intersalar Range lavas. Field of view is approximately 2 mm for each image. (A) Highly porphyritic lava from Pliocene Cerro Grande lavas (sample #15) with phenocrysts of plagioclase and amphibole, typical of silicic composite centers. (B) Olivine phenocryst and groundmass from the Pliocene phenocryst-poor trachyandesite Jachcha Pallallí torta (sample #32), typical of lavas from the relatively mafic monogenetic centers of the central Altiplano. (C) Olivine-bearing basaltic trachyandesite from the Pliocene Coracora center (sample #42). (D) Miocene rear arc amphibole- and biotite-bearing trachyandesite lavas of Cosoxaya (Sample #68).

(Figures 8A–D), K_2O is positively correlated, and Na_2O and MnO show little to no variation.

Overall, major and trace element compositions (Supplementary Material, Figure 8) of Intersalar Range lavas show broad similarities with the CVZ arc, with the notable exceptions of the Intersalar Range lavas containing significantly higher concentrations of Nb, Ta, and TiO_2 . Considering the entire geochemical suite: Rb, Pb, Th, Y, U, and Cs are positively correlated with silica, whereas Sr, Ni, Cr, V, Cu, Zn, Sc, Sm, and Eu are negatively correlated. In contrast, the high field strength elements (HFSEs), notably Nb, and all other analyzed trace elements show little to no correlation with silica. All Intersalar Range lavas are characterized by typical arc-

like trace element signatures with enrichments in Rb, Ba, Th, and K and relative depletions in Nb, Ta, and Ti compared to N-type MORB (Figure 9A). On a chondrite normalized rare earth element (REE) diagram, the younger volcanoes are characterized by steeper slopes and correspondingly higher normalized La/Yb ratios (Figure 9B). Variations in major and trace element data were analyzed with respect to both age and across-arc distance, measured here as distance from the Peru-Chile trench, with the most notable observations shown in Figure 10. These systematic geochemical differences are evaluated below in the Discussion section.

In Intersalar Range samples, $^{87}Sr/^{86}Sr$ values (0.70512–0.70600) show a much smaller range compared to



¹⁴³Nd/¹⁴⁴Nd (0.51226–0.51255) (Figure 11). Many of the ⁸⁷Sr/⁸⁶Sr values are lower compared to the nearby CVZ arc of the northern Altiplano (Parinacota to Ollagüe) and are significantly lower than the lavas of the eastern Altiplano and the large-volume ignimbrite centers of Los Frailes and the Altiplano-Puna Volcanic Complex. ¹⁴³Nd/¹⁴⁴Nd values of the Intersalar Range sample set tend to be somewhat higher than the eastern Altiplano lavas and ignimbrite complexes. In the reararc volcanoes of the Intersalar Range, ⁸⁷Sr/⁸⁶Sr values generally increase, and ¹⁴³Nd/¹⁴⁴Nd values decrease, from the Miocene to the Plio-Pleistocene with some exceptions (Figures 12A,B). ⁸⁷Sr/⁸⁶Sr values show little correlation with distance from the arc in either age group (Figure 12D), whereas ¹⁴³Nd/¹⁴⁴Nd values of the western Miocene samples are higher than those in the east (Figure 12E). With increasing SiO₂, ⁸⁷Sr/⁸⁶Sr and ¹⁴³Nd/¹⁴⁴Nd show only moderate positive and negative correlation, respectively. ²⁰⁶Pb/²⁰⁴Pb, ²⁰⁷Pb/²⁰⁴Pb, and ²⁰⁸Pb/²⁰⁴Pb values of Intersalar Range samples range from 17.7315–18.5095, 15.5714–15.6279, and 37.7862–38.6156, respectively. The

²⁰⁶Pb/²⁰⁴Pb values are consistent with Mamani et al. (2010) and nearly all fall within the range of the Arequipa crustal domain (16.083 < ²⁰⁶Pb/²⁰⁴Pb < 18.453) with two of the samples plotting just outside the Arequipa field. Among the reararc samples, Pb isotope values show significantly more systematic variation with respect to east/west distance from the arc (Figure 12F) than with age (Figure 12C). Pb isotopes of Intersalar Range samples show no systematic variation with SiO₂.

Discussion

The new dataset presented in this study allows an evaluation of the timing and processes of magmatism in the Intersalar Range of western Bolivia and its relationship to the development of the Central Andean Plateau. Below, we use the term ‘arc’ volcanism to refer to typical subduction volcanism related to dehydration of the subducting oceanic plate and “non-arc” volcanism to refer to any

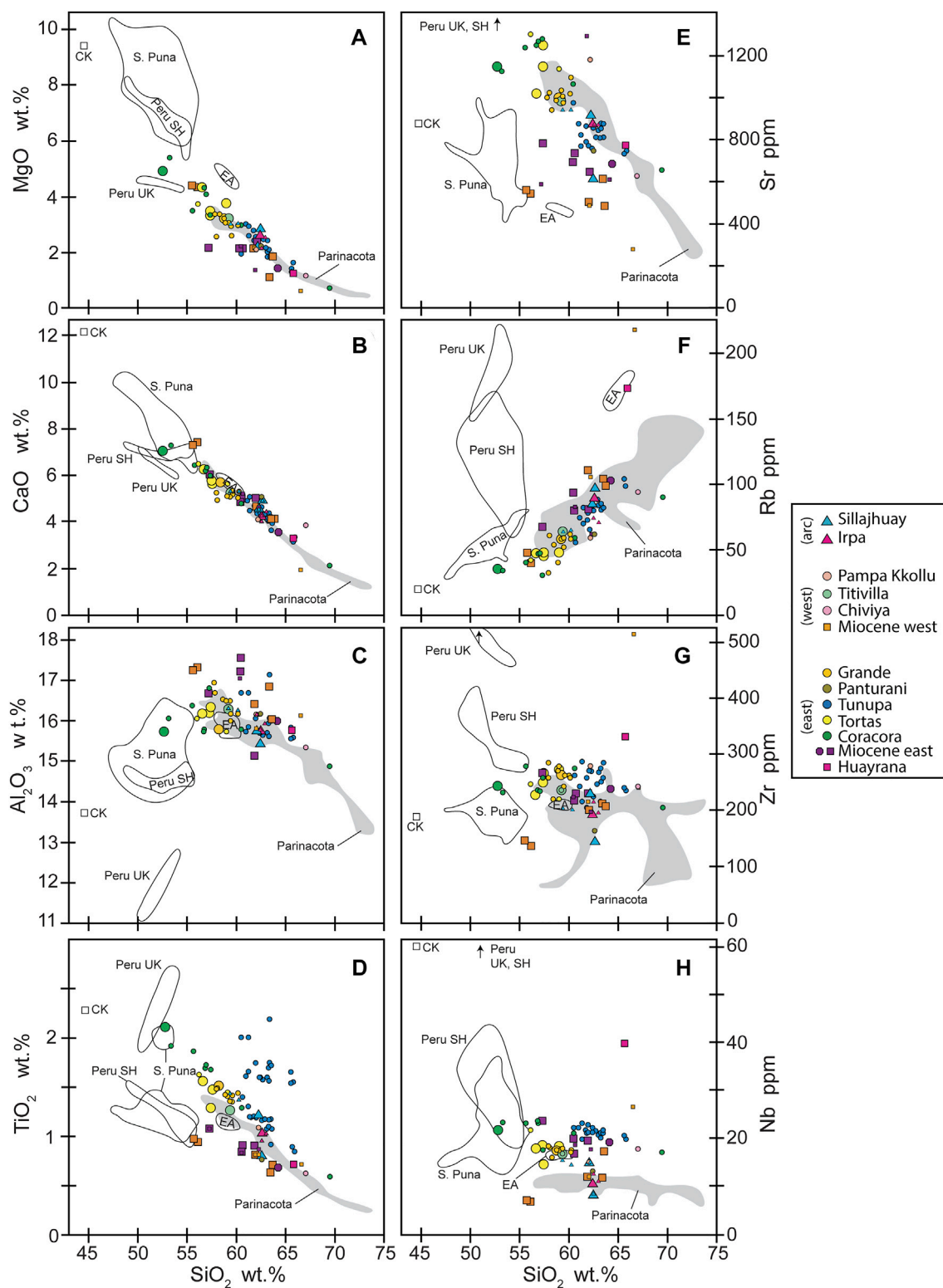


FIGURE 8
 Selected Harker diagrams of Intersalar Range lavas. Compositional field of Parinacota volcano shown for comparison to a well-studied CVZ composite volcano of the main arc (Hora et al., 2009). Select reararc lavas of the plateau are also shown for comparison (same references as Figure 7). Reararc TiO₂ and Nb values exhibit the largest deviation from the Parinacota array. Note that shoshonitic (SH) and ultrapotassic (United Kingdom) lavas from the Peruvian reararc (Carlier et al., 2005) are extremely enriched in trace elements and plot off the diagrams of Sr, Zr, and Nb. Larger symbols from the current study represent data with ⁴⁰Ar/³⁹Ar age control.

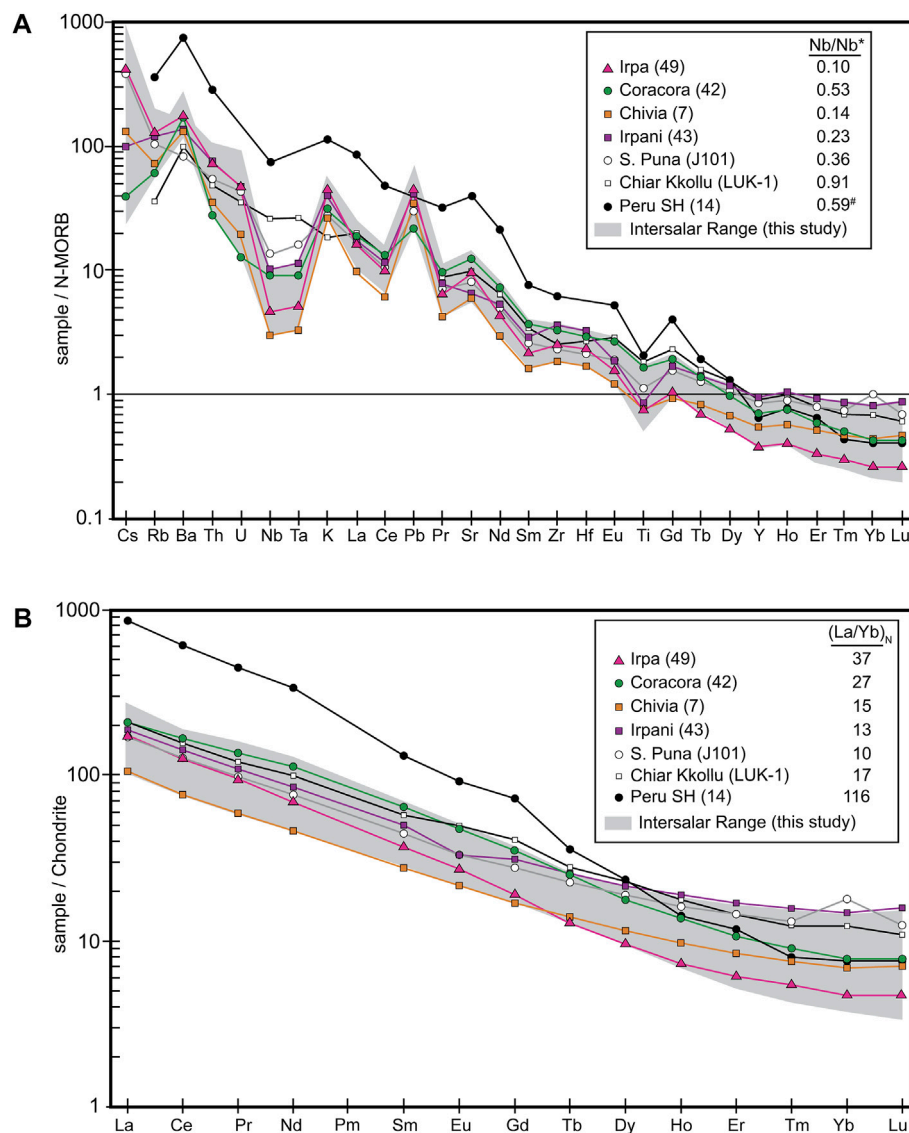


FIGURE 9

Normalized abundances (Sun and McDonough, 1989) of trace elements for representative Intersalar Range samples: Plio-Pleistocene arc (Irpa) and reararc (Coracora); Miocene arc (Chivia) and reararc (Irpani). Prominent reararc lavas shown for reference and discussed in text (references as in Figure 7). Sample numbers in parentheses. (A) Spidergram showing incompatible element enrichment patterns relative to the primitive mantle. Notice the wide range in Nb and Ta values. The depth of the negative Nb anomaly shown as values of Nb/Nb*, calculated relative to U and K (#note that Peru shoshonites were not analyzed for U and the value of Nb/Nb* is calculated based on the curve of the pattern shown on this graph). Reararc lavas of both Plio-Pleistocene and Miocene lavas are characterized by smaller negative Nb anomalies (higher Nb/Nb* values) compared to the arc. (B) Chondrite-normalized REE patterns. In contrast to Nb/Nb*, the most pronounced differences in REE patterns correlate with age: Pliocene-Pleistocene samples (e.g., Irpa and Coracora) are characterized by steeper slopes and higher La/Yb ratios compared to the Miocene samples (e.g., Chivia and Irpani).

other type of magmatic trigger. Arc volcanism along the western edge of central South America extends to at least the Jurassic and has been more or less continuous in the Western Cordillera at the latitude of the Intersalar Range since the Late Oligocene, following an ~10 m.y. Volcanic hiatus between ~35 and 25 Ma that is attributed to an episode of flat-slab subduction (James and Sacks 1999). Although it is unresolved precisely how far arc volcanism

extends eastward into the reararc region, we consider typical subduction-related flux melting unlikely to explain the entirety of Intersalar Range volcanism due to the large distances (>100 km) from the arc front. We also consider the hypothesis of decompression melting and lateral melt migration from beneath Los Frailes (Hoke and Lamb, 2007) as an implausible explanation for the volcanoes of the central Altiplano including those of the eastern

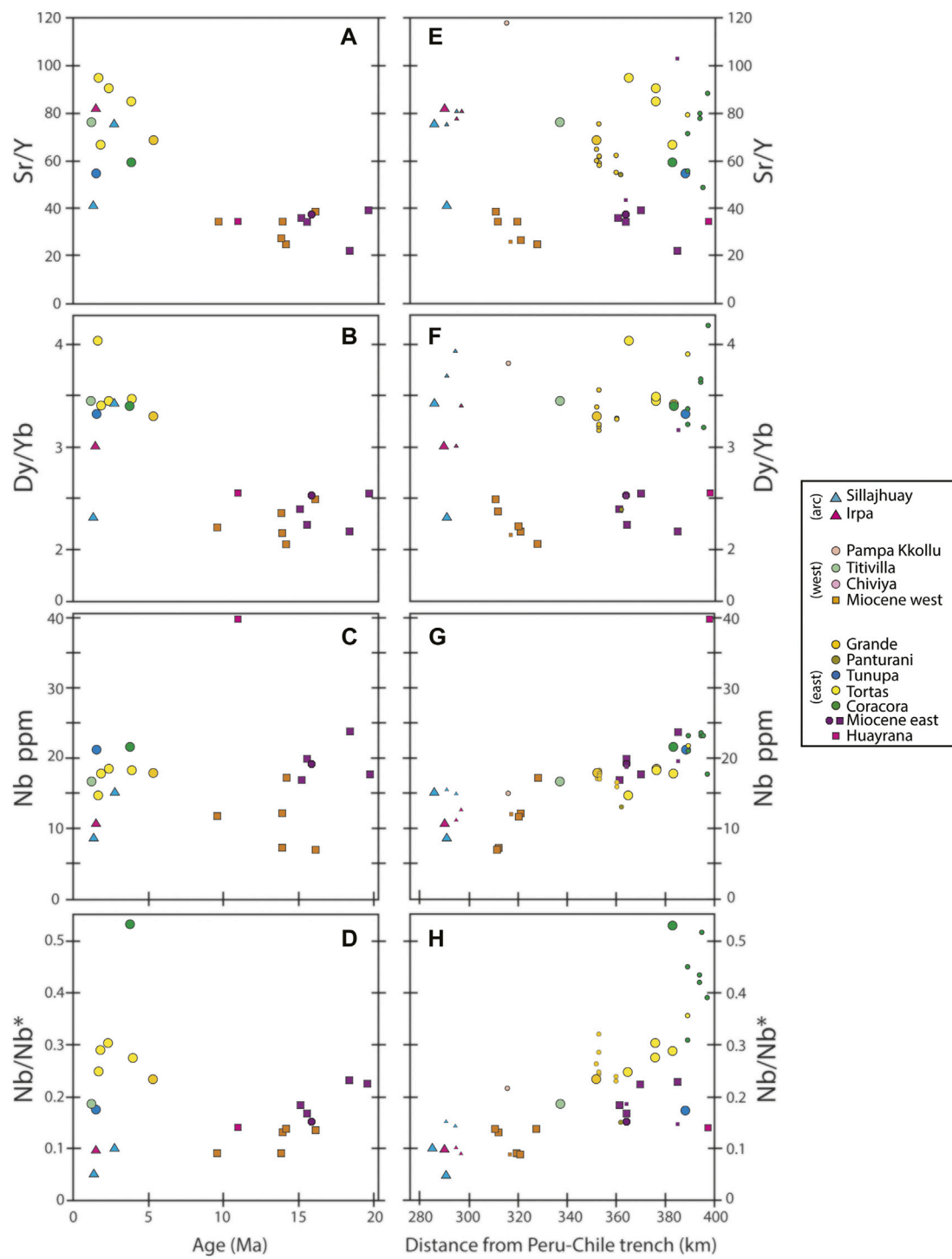


FIGURE 10

Geochemical data from the Intersalar Range plotted against age (A–D) and distance from the Peru-Chile trench (E–H). Larger symbols indicate samples with $^{49}\text{Ar}/^{39}\text{Ar}$ age control. Nb exhibits the best correlation with distance for all elements analyzed. Nb/Nb* is a measure of the depth of the negative Nb anomaly compared to U and K. See text for details.

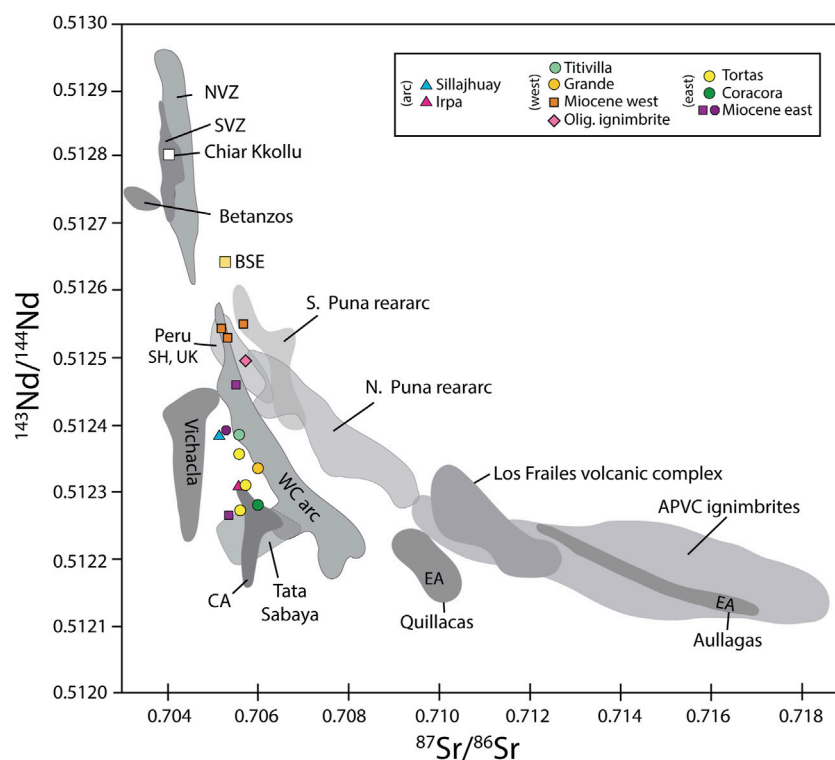


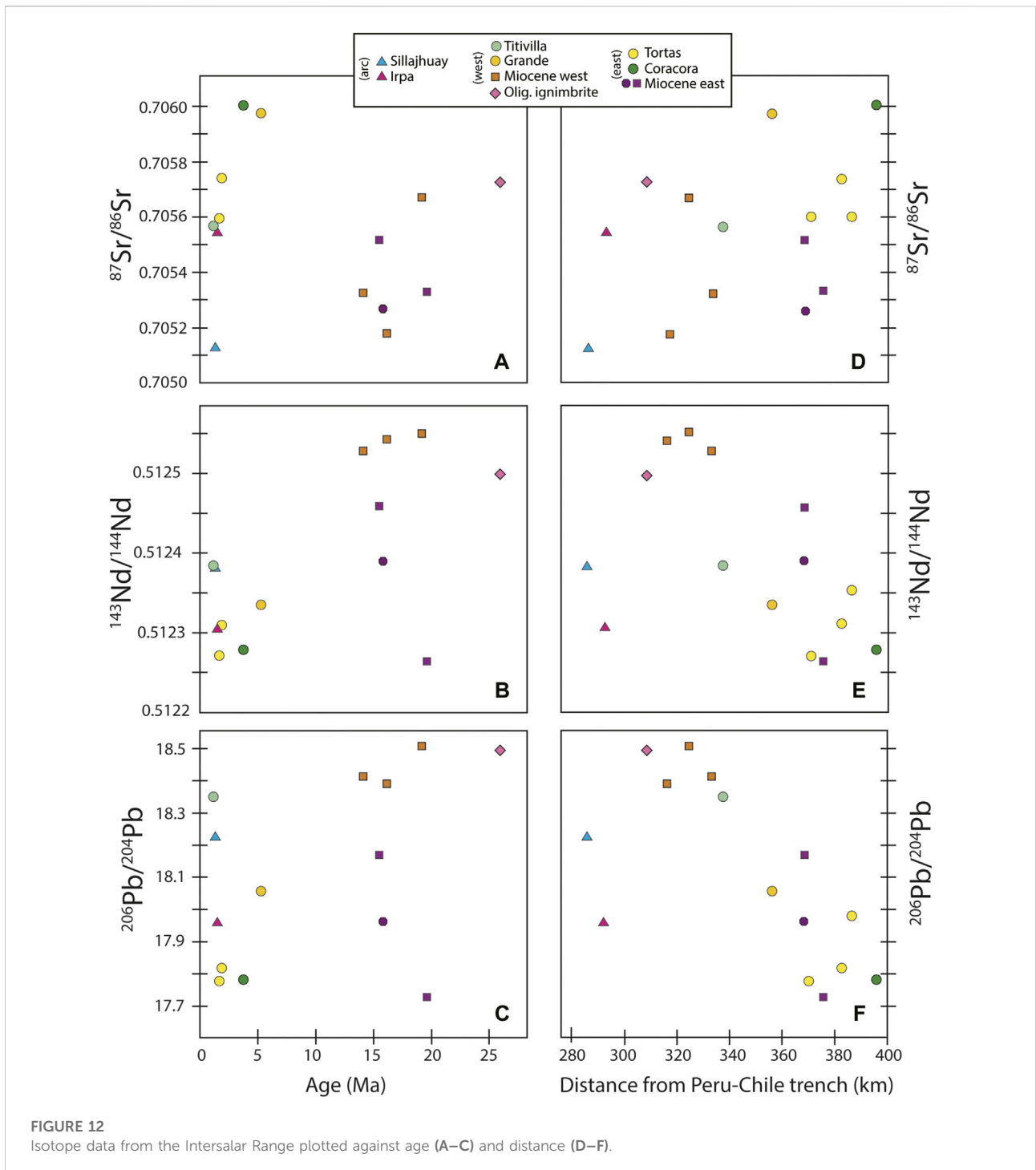
FIGURE 11

$^{87}\text{Sr}/^{86}\text{Sr}$ and $^{143}\text{Nd}/^{144}\text{Nd}$ data from the Intersalar Range with select Central Andean igneous rocks for reference. The Western Cordillera (WC) arc array includes Pleistocene centers of Pomerape, Irruputuncu, El Rojo Norte, Olca (Mamani et al., 2010); Aucanquilcha, La Poruñita (Walker 2011); and Ollagüe (Feeley and Davidson, 1994). Reararc centers include Tata Sabaya (de Silva et al., 1993); Chiar Kkollu and other small volume mafic rocks of the central Altiplano (CA; Davidson and de Silva, 1995) and eastern Altiplano (EA; McLeod et al., 2012). Reararc mafic rocks from the central Altiplano (Chiar Kkollu southern Puna in Argentina (Kay et al., 1994; Drew et al., 2009; Risse et al., 2013), the northern Puna in Argentina (Maro et al., 2017), and the northern Altiplano in Peru (Carlier et al., 2005) are shown for reference. Northern Volcanic Zone (NVZ) and Southern Volcanic Zone fields compiled from the GeoROC database 2012 (<http://georoc.mpch-mainz.gwdg.de/georoc>). Cretaceous rifting-related volcanism of Betanzos and Vichacla from the Bolivian Eastern Cordillera (Lucassen et al., 2007), and the dominantly crustal-derived ignimbrites of Los Frailes (Kato, 2013) and the Altiplano Puna volcanic complex (Lindsay et al., 2001; Kay et al., 2010) are also shown for comparison. Bulk Silicate Earth (BSE) from Rollinson (1993).

Intersalar Range. Such a model would require the lateral melt migration of more than 100 km and is also inconsistent with the apparent pulsing of magmatism in the Intersalar Range, in contrast with the more consistent eruptions of the Los Frailes region since the Early Miocene (Figure 13B).

The onset of widespread reararc volcanism at ~25 Ma across much of the footprint of the Central Andean Plateau, is strongly suggestive of a causal relationship between reararc magmatism and the physical processes related to plateau construction (James and Sacks, 1999; Trumbull et al., 2006). The most likely hypothesis of a reararc melting trigger in the Central Andean Plateau is related to delamination, or foundering, of the mantle lithosphere and mafic lower crust (e.g., Kay and Kay, 1993; Allmendinger et al., 1997; DeCelles et al., 2015). However, the details related to the timing, scale, and mechanisms of foundering remain unconstrained. Removal of the lower crust and lithosphere can induce magmatism by multiple mechanisms, including return flow of the asthenosphere

(decompression melting) around the foundering block; conductive heating of the foundering and/or newly exposed mantle lithosphere and crust; and dehydration melting of the asthenosphere and/or mantle lithosphere caused by the pressure-induced breakdown of hydrous minerals as the block descends to greater pressures and depths (e.g., Elkins-Tanton, 2005). In the case of dehydration melting, an arc-like trace element signature would be expected. Assimilation of crust previously generated in an arc setting would also imprint an arc signature. Due to the thick continental crust of the Central Andes, significant amounts of magma storage, assimilation, and fractional crystallization likely occurs at multiple levels in the crust, regardless of the original melting mechanism. Consequently, it can be difficult to unravel arc and non-arc magmatic processes in the Central Andes and it is within this context that we evaluate the spatial, temporal, elemental, and isotopic differences within the Intersalar Range to search for clues into the underlying magmatic sources and melting triggers.



Volcanism, deformation, and crustal thickening in the Intersalar Range

The apparent pulsing of magmatism in the eastern Intersalar Range (>100 km from the contemporaneous arc front) in the Miocene and the Plio-Pleistocene is consistent with at least two separate melting events, most likely related to partial removal of the

mantle lithosphere and lower crust. The first pulse began with the relatively low-volume eruptions of Cosoxaya and Irpani in the Early Miocene and continued with a larger flux of volcanism in the same region between ~14 and 16 Ma with the eruption of lavas of the Huaña Amata composite center. This larger flux of volcanism may also include significant volumes of explosive volcanism as evidenced by two coincident K/Ar ages reported by [Leytón and Jurado \(1995\)](#)

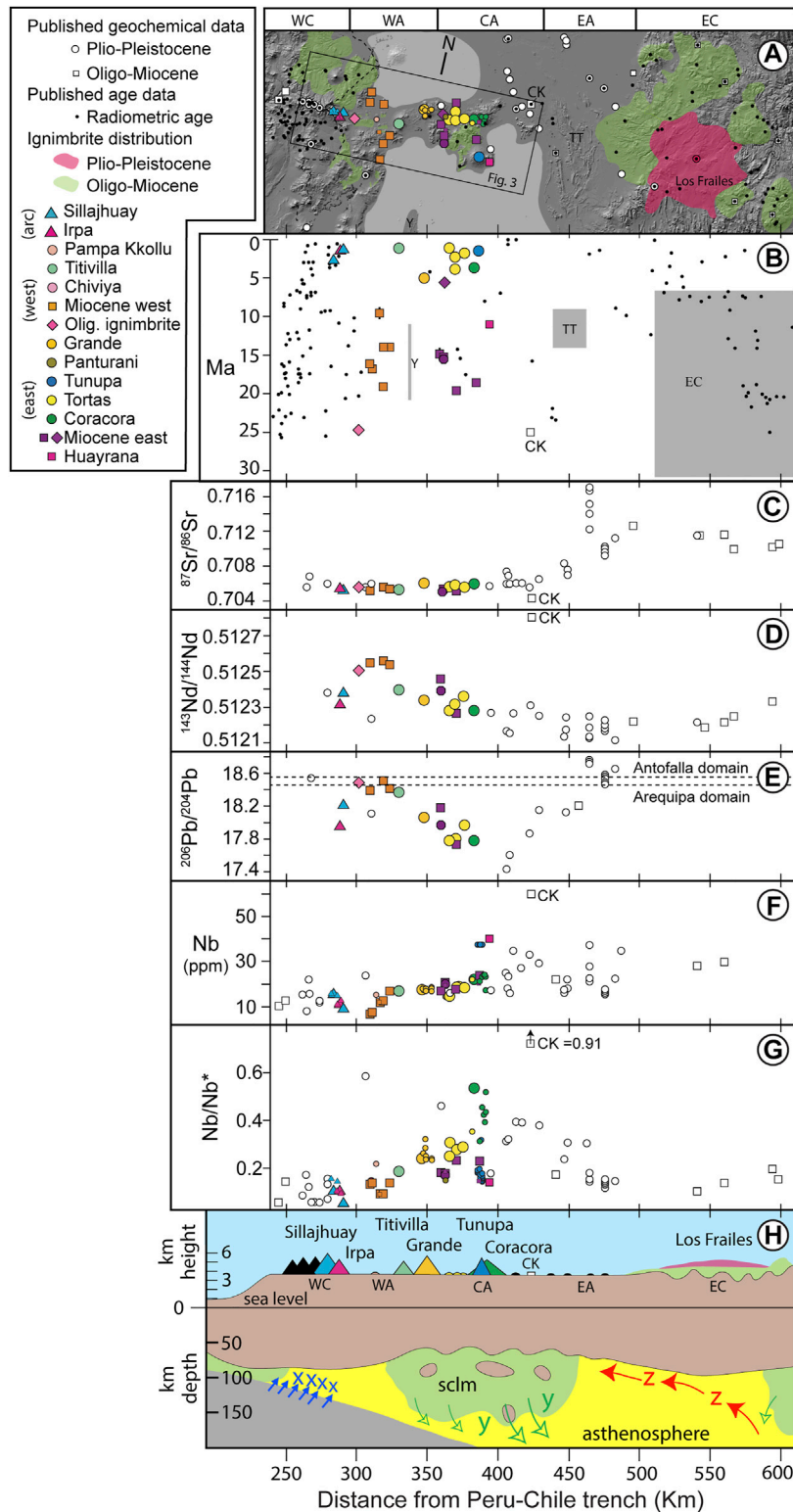


FIGURE 13

Arc-perpendicular compilation of available data collected within the larger bounding box of Figure 1. Note that north is offset approximately 12.5° to align perpendicular to the Peru–Chile trench and the trend of the CVZ arc (See Figure 1). Colored symbols from this study and Salisbury et al. (2015); larger symbols indicate samples with $^{49}\text{Ar}/^{39}\text{Ar}$ age data. Compositional data are restricted to <66 wt% SiO₂. (A) Sample localities of this study and all available published data within the confines of the image. The horizontal axis is shown in (H) and is the same in all graphs. WC, Western (Continued)

FIGURE 13 (Continued)

Cordillera, WA, western Altiplano, CA, central Altiplano, EA, eastern Altiplano, EC, Eastern Cordillera, CK, Chiar Kkollu, Y, Yazón Anticline, TT, Tambo Tambillo fold and thrust belt. (B) Compilation of data from this study and published radiometric age data (Evernden et al., 1977; Grant et al., 1979; Almendras, 2002; Aitchison et al., 1995; Kato, 2013; and references of Figure 4), sample localities shown in (A). Shaded areas represent timing and width of exposed surface deformation of the Yazón anticline (Elger et al., 2005), Tambo Tambillo fold and thrust belt (Kennedy et al., 1995) and the Eastern Cordillera (McQuarrie et al., 2005). (C–E) $^{87}\text{Sr}/^{86}\text{Sr}$, $^{143}\text{Nd}/^{144}\text{Nd}$, and $^{206}\text{Pb}/^{204}\text{Pb}$ isotope data from this study and published data (same references as Figure 11). The Pb isotope domains (based on Pb isotope values, not location) of Mamani et al. (2010) are shown for reference in (E). (F) Nb concentrations plotted against distance from trench showing distinct eastward increase from the CVZ arc to the central Altiplano. Published data with multiple datapoints for single centers are shown as averages. (G) Nb/Nb* values plotted against distance from Peru–Chile trench. Higher values indicate smaller negative Nb anomalies. The highest Nb/Nb* values are found within igneous rocks of the central Altiplano and correlate spatially with the presence of the intact mantle lithospheric root shown in (H). (H) Schematic cross section across the Central Andean Plateau showing proposed dominant melting triggers beneath each region. X = dehydration of subducting Nazca plate; y = foundering of subcontinental lithospheric mantle (sclm) and lower crust; Z = decompression melting of upwelling asthenosphere as described by Hoke and Lamb (2007). Following Hoke and Lamb (2007), foundering of the mantle lithosphere beneath the Eastern Altiplano/Eastern Cordillera likely occurred following the end of flat-slab subduction ~25 Ma. Lithospheric structure after Beck and Zandt (2002).

for the extensive ignimbrites of Chorca and Mokho. An apparent ~8 m.y. Hiatus of significant volcanism in the eastern Intersalar Range was then followed by the second pulse of magmatism, represented by eruptions of the Grande, Coracora, Tunupa, and the monogenetic tortas.

The timing of the Miocene pulse of volcanism in the Intersalar Range overlaps with deformation of the Yazón Anticline (Figure 13B), suggesting a possible relationship between these two events. There is no temporal relationship between Plio-Pleistocene volcanism and surface structures in the region. Trace element data are consistent with significant crustal thickening following the Miocene pulse and preceding the Plio-Pleistocene pulse. Higher Sr/Y values are recorded in the Plio-Pleistocene lavas compared to the Miocene samples in both the western and eastern parts of the range, with little to no observed spatial variation in either age group (Figures 10A,E). These higher values suggest magma equilibration in the presence of garnet and absence of plagioclase at the base of significantly thicker crust in the Plio-Pleistocene compared to the Miocene (e.g., Kay et al., 1994). Higher Dy/Yb in the Plio-Pleistocene group (Figure 10B) is also consistent with an increasing role of garnet, as opposed to amphibole, in the fractionation of the younger lavas. A thicker crust in the Plio-Pleistocene is further supported by steeper, chondrite-normalized REE patterns and higher $[\text{La}/\text{Yb}]_{\text{N}}$ values (Figure 9B), further indicating an increasing role of garnet fractionation in the younger samples. As the 9.49 ± 0.77 Ma Picacho lavas plot with the older samples, the crustal thickening implied by the trace element data likely occurred after this time. Figures 12A,B shows an apparent increase in $^{87}\text{Sr}/^{86}\text{Sr}$ and decrease in $^{143}\text{Nd}/^{144}\text{Nd}$ in the Plio-Pleistocene samples compared to the Miocene samples, although overlap is observed. This result is consistent with increased assimilation of continental crust in the younger, thicker crust. No systematic variations in Pb isotopes were observed between the two age groups. As the Late Miocene crustal thickening implied by the trace element data apparently occurred in the absence of local surface deformation, lower crustal flow from deformation of the Tambo Tambillo region (~14–5 Ma) and/or from the Eastern Cordillera (Husson and Sempere, 2003) may be invoked to resolve this discrepancy. The ductile flow of crust and, presumably, the mantle lithosphere below, is also consistent with the proposed

foundering magmatic trigger of the Plio-Pleistocene volcanism of the eastern Intersalar Range.

Spatiotemporal and geochemical variations across the Intersalar Range and the Central Andean Plateau

To determine which elements showed the strongest east-west variation across the Intersalar Range, we plotted the concentration of all analyzed major and trace elements against distance from the Peru–Chile trench and quantified the correlations through least squares (r -squared) analysis. Only samples with age control and $\text{SiO}_2 < 63$ wt% were used in these calculations. Our results indicate that although overall systematic trace element variations across the Intersalar Range are limited, select elements, particularly Nb and other HPSEs, do show significant east-west correlations. For the Plio-Pleistocene group, Nb ($r^2 = 0.75$) shows the strongest correlation with distance from the trench and, thus, the arc front. For the Miocene group, the Nb correlation ($r^2 = 0.83$) is second only to Eu. Consequently, in the Plio-Pleistocene group, any ratio with Nb in the numerator increases with eastward distance in the Intersalar Range, and any ratio with Nb in the denominator will decrease. This observation suggests that the Nb values are not primarily controlled by lower amounts of partial melting in the reararc. The relative increase in Nb concentrations relative to other trace elements into the reararc is further demonstrated by correspondingly decreasing depths of the negative Nb anomaly on mantle-normalized spidergrams of Intersalar Range lavas (Figure 9A). The Nb anomaly can be quantified through calculation of Nb/Nb*, measured as the depth of the Nb anomaly relative to the adjacent LILEs of U and K. It is calculated here as $[\text{Nb}/\text{Nb}^* = \text{Nb}_{\text{N}}/(\text{U}_{\text{N}}^{2/3} * \text{K}_{\text{N}}^{1/3})]$ where Nb_{N} , U_{N} , and K_{N} are the mantle-normalized (Sun and McDonough, 1989) values of Nb, U, and K, respectively; as for a similar calculation for Dy/Dy* by Davidson et al. (2007). We note that the choice of nearby trace elements to make this calculation makes little difference in the across-arc calculations of Figure 10H as Nb increases in the reararc are higher relative to all other trace elements analyzed.

Figure 10H demonstrates the significant increase of Nb/Nb* into the reararc in the Plio-Pleistocene samples, and to a lesser extent in the Miocene group. In the Plio-Pleistocene samples, no systematic east-west variations in isotopic ratios are observed, and only moderate differences are observed in the Miocene samples in $^{143}\text{Nd}/^{144}\text{Nd}$ and $^{206}\text{Pb}/^{204}\text{Pb}$.

To better comprehend the spatiotemporal and geochemical differences across the Central Andean Plateau, we extended our across-arc analysis to include available published data between $\sim 19\text{oS}$ and 21.6oS , spanning the Western Cordillera, Altiplano, and Eastern Cordillera and compare these data with a schematic cross section of the lithospheric structure modified from Beck and Zandt (2002) based on geophysical and geological studies at the latitude of the study area (Figure 13). The most intriguing result of this analysis is the correlation observed between the highest Nb/Nb* values of the Plio-Pleistocene lavas and the location of the mantle lithosphere root identified by Beck and Zandt (2002) beneath the central Altiplano (Figures 13G,H). In contrast, lower Nb/Nb* values (stronger negative Nb anomalies) correlate with the arc front of the Western Cordillera and the far reararc of the eastern Altiplano and Eastern Cordillera, both regions where subcontinental lithosphere mantle is hypothesized by Beck and Zandt (2002) to be absent. We note that the overall conical shape of this pattern is apparent in the relatively more mafic rocks of the tortas, Coracora, and the monogenetic flows of the central and eastern Altiplano, suggesting that fractionation of K and U is not a major factor. This observation is supported by the overall concentrations of Plio-Pleistocene Nb values, which are significantly higher in the eastern Intersalar Range lavas compared to the west (Figures 9A, 10G), and show almost no variation with wt% SiO_2 in the Intersalar Range (Figure 8H) or within individual centers (Salisbury et al., 2015).

Pb isotope values also appear to show a correlation with the presence of subcontinental mantle lithosphere as samples with the lowest $^{206}\text{Pb}/^{204}\text{Pb}$ are located in the central Altiplano (Figure 13E). $^{87}\text{Sr}/^{86}\text{Sr}$ values vary very little from the arc to the central Altiplano and are significantly higher in the east where the mantle lithosphere is absent (Figure 13C), including within the relatively mafic, olivine-bearing monogenetic centers of the eastern Altiplano (Davidson and de Silva, 1995; McLeod et al., 2013) and the ignimbrites of the Los Frailes volcanic complex (Kato, 2013). $^{143}\text{Nd}/^{144}\text{Nd}$ values are highest in the Intersalar Range, particularly in the Miocene samples, and are generally lower in the eastern Altiplano and Eastern Cordillera (Figure 13D).

Petrogenesis of Intersalar Range magmatism

Based on the spatial, temporal, and geochemical variations of this study and of those across the plateau, we consider the hypothesis of piecemeal foundering of enriched mantle lithosphere and eclogitized lower crust beneath the central Altiplano during the Miocene, and again during the Plio-Pleistocene, as the most likely explanation of reararc volcanism in the Intersalar Range. This

hypothesis is primarily supported by the apparent pulsing of magmatism in the eastern Intersalar Range, and systematic differences in geochemistry between the arc and reararc regions, including elevated Nb and Nb/Nb* values in the eastern Intersalar compared to the western portion of the range and the arc front (Figure 9A, 10G-H, 13F-G). We expand on the model of Salisbury et al. (2015), which interpreted the anomalously high Nb concentrations of Tunupa volcano to reflect a significant component of the mantle lithosphere and suggested that the breakdown of the hydrous phases of amphibole and phlogopite as most likely responsible for the Nb signal. In this model, hydrous minerals such as amphibole and phlogopite strongly concentrate Nb-Ta-Ti during episodes of flat-slab subduction and metasomatism of the mantle lithosphere. Although HFSE are thought to be largely residual during slab dehydration, Nb-Ta-Ti may concentrate in hydrous minerals over multiple episodes of flat-slab subduction over 10s or 100s of millions of years. When the thickened mantle lithosphere and garnet-bearing lower crust become gravitationally unstable, detach, and founder (delaminate) into the asthenosphere, the increasing pressure forces the breakdown of amphibole and phlogopite, triggering wet melting and releasing their Nb-enriched trace element load. As vein amphibole in mantle xenoliths found elsewhere can contain higher concentrations of Nb and Ta relative to primitive mantle compared to all other trace elements, including K (Ionov et al., 1997), we consider this phase the most probable to control the observed Nb signal in the Intersalar Range and the broader arc-normal transect (Figure 13F). Fractionation of Ti-oxides such as rutile may also play a role in the Nb-Ta-Ti systematics, however, amphibole, and to a lesser extent phlogopite, are by far more common in mantle xenoliths in alkali basalts (Ionov et al., 1997). Cenozoic mantle xenoliths are essentially absent in the Cenozoic Central Andes (Lucassen et al., 2005), however, the extremely high Nb (>100 ppm) and Nb/Nb* values (>1) of Cretaceous-aged, extension-related alkaline magmatism from Ayopaya, Betanzos, and Vichacla (Schultz et al., 2004; Lucassen et al., 2007) in what is now the Eastern Cordillera of Bolivia suggest that the mantle lithosphere was already strongly metasomatized prior to the most recent flat-slab subduction between ~ 35 and 25 Ma. Partial removal of the lower lithosphere likely also triggers decompression melting in the upwelling asthenosphere. Following Blume-Oeste and Wörner (2016), we consider the lavas of the eastern Intersalar Range to be derived from a mixture of the mantle lithosphere and the convecting mantle asthenosphere, which then further assimilate and homogenize within the continental crust. Identification of precise compositions and the relative volume of endmember components is challenging as the few mafic magmas that erupted on the Central Andean Plateau are scattered across the plateau, and the composition of the mantle lithosphere, asthenosphere, and crust likely vary in both space and time.

We propose that Nb is particularly useful in recognizing a significant component of the mantle lithosphere even in magmas that are heavily influenced by crustal processing. Magmas thought to

be derived from the mantle lithosphere are typically alkaline and defined by distinct Nb enrichments relative to most other trace elements (e.g., Pilet et al., 2008). In the Intersalar Range dataset, the basaltic trachyandesites from Coracora and the trachyandesitic monogenetic tuffites west of Coracora, provide the strongest evidence for magmas with a significant component of enriched mantle lithosphere as a result of melting related to lithospheric foundering. The Coracora lavas erupted ~130 km east of the contemporaneous arc front (Figures 4, 13A, Figures 13B), are slightly alkaline (Figure 7), relatively high in TiO₂ (Figure 8D), and are characterized by the highest Nb/Nb* values analyzed in this study (Figures 9A, 10H). The mafic, isotopically depleted, trace-element enriched, ~25.1 Ma Chiar Kkollu sill (Davidson and de Silva, 1995; Hoke and Lamb, 2007) located in the central Altiplano ~20 km east of the Intersalar Range (Figures 1, 3) may represent the least-contaminated endmember of mantle lithosphere-derived magmatism in the Bolivian Altiplano, and data from this sample are shown in Figures 4, 7–9, 11, 13 for comparison with the newly collected data of this study. Chiar Kkollu has the highest measured Nb concentrations (60 ppm) and the highest Nb/Nb* values (0.91) of the Bolivian Altiplano and is also situated above the partially intact mantle lithospheric root of the central Altiplano (Figures 13F–H).

Elsewhere in the Central Andean Plateau, elevated Nb and Nb/Nb* values are observed in mafic lavas of the southern Puna of Argentina (Drew et al., 2009; Risse et al., 2013), and the phlogopite-bearing shoshonites and ultrapotassic mafic lavas of the northern Altiplano of Peru (Carlier et al., 2005), both of which show little to no evidence of crustal contamination and are interpreted to derive from the mantle lithosphere. The mafic rocks of the southern Puna of Argentina have long been hypothesized to be the result of lithospheric delamination (e.g., Kay and Kay, 1993; Kay et al., 1994; Drew et al., 2009; Murray et al., 2015) and we suspect a similar process in the central Altiplano of Bolivia, although with more crustal contamination in the Bolivian samples. The southern Puna and northern Altiplano rear arc lavas are plotted in Figures 7–9, 11 to demonstrate the geochemical similarities with the lavas of the eastern Intersalar Range, particularly those of Coracora volcano.

Alternatively, or additionally, the source of the observed high Nb concentrations could be influenced by the breakdown of an amphibole-rich “sponge” that had accumulated in the middle to lower crust (Davidson et al., 2007), which filters these elements in addition to water. However, in volcanoes such as Mount Pelée where “cryptic amphibole fractionation” is suspected due to decreases in Dy/Yb with increasing SiO₂ (Davidson et al., 2007) a corresponding decrease in Nb is not observed, suggesting that Nb is not strongly concentrated in amphibole at crustal pressures. Furthermore, crustal compositions of exposed Andean basement and crustal xenoliths are typically lower in Nb concentrations than those observed in the central Altiplano lavas (e.g., Lucassen et al., 2005), suggesting that the mantle lithosphere is most likely responsible for the observed Nb signature in Intersalar Range lavas. Evidence against a crustal influence for the observed Nb signal is also found in the lack of north-south Nb and Nb/Nb* variations in lavas erupted on either side of the of the Pb-

isotope-defined crustal boundary along the Quaternary CVZ arc (Aitchison et al., 1995; Mamani et al., 2010), suggesting that the distinct crustal domains are not strongly affecting Nb trends.

The variations in Sr-Nd-Pb isotopes observed in this study preclude a simple interpretation with respect to the mantle source regions across the Intersalar Range and the broader plateau transect. Despite the limitations, the isotopic data show some consistency with our hypothesized petrogenetic model. A correlation is observed between Pb isotope values and the presence of the lithospheric root beneath the central Altiplano (Figure 13E), although these variations exist within the field of the Arequipa domain of Mamani et al. (2010) and may also be explained by local variations in the age of the contaminated continental crustal. The relatively low ⁸⁷Sr/⁸⁶Sr and somewhat high ¹⁴³Nd/¹⁴⁴Nd values of the Intersalar Range compared to other rear arc lavas of the Central Andean Plateau (Figures 13C,D) are consistent with a component of mantle lithosphere as evidenced by correspondingly low ⁸⁷Sr/⁸⁶Sr and high ¹⁴³Nd/¹⁴⁴Nd values of regional magmas suspected to be derived from the mantle lithosphere, including those of Betanzos and Vichacla in Bolivia (Lucassen et al., 2007), and the shoshonites and ultrapotassic lavas of the Peruvian rear arc (Carlier et al., 2005) (Figure 11). However, significant overlap in these values with lavas from the arc is also observed and we note that lavas from Coracora are characterized by the lowest ¹⁴³Nd/¹⁴⁴Nd values analyzed in this study. Despite a significant shift in Sr isotope values at the boundary between the central and eastern Altiplano, no clear correlation with the mantle lithosphere root in the central Altiplano is apparent in the data in either the Sr or Nd isotope data (Figures 13C,D). We suggest that in the absence of mafic magmatism and a correspondingly definitive isotopic signature, Nb and Nb/Nb* values may be useful in identifying a significant component of mantle lithosphere. Nb (and to a lesser extent Ta and Ti), may be one of the few elements that can effectively “see through” the effects of crustal contamination in silicic rocks and can aid in the identification of primary characteristics of the underlying mantle source.

Conclusion

The Intersalar Range provides a unique opportunity to assess a temporally constrained transect spanning the arc and rear arc regions of the Bolivian Altiplano. Twenty-three new ⁴⁰Ar/³⁹Ar age dates reveal a discontinuous eruptive history in the rear arc region with primary magmatic phases in the Miocene (~20–11 Ma, dominantly between 14–16 Ma) and the Plio-Pleistocene (~5–1 Ma). The distinct eruptive phases contrast with the more continuously active volcanism in the Western and Eastern Cordilleras and are suggestive of distinct, non-arc magmatic triggers beneath the central Altiplano at these times. We interpret these data within the context of previous studies (e.g., Beck and Zandt, 2002; Barnes and Ehlers, 2009; Drew et al., 2009) which favor a model of localized, piecemeal foundering events over the timespan of construction of the Central Andean Plateau to explain the relative lack of mantle lithosphere and

lower mafic crust, and the apparent slow and steady uplift of the plateau. Although the Miocene volcanism coincides temporally with surface deformation to the south of the Intersalar Range, significant crustal thickening between ~9.5 Ma and ~5 Ma is implied by elevated Sr/Y, Dy/Yb, and [La/Yb]_N in the Plio-Pleistocene samples, consistent with ductile lower crustal flow as a mechanism to thicken the crust and to promote lithospheric foundering. Relatively high Nb concentrations (>~15 ppm) compared to the arc, and high Nb/Nb* values (>0.3) correlating with the presence of intact mantle lithosphere beneath the central Altiplano, are interpreted as reflecting dehydration melting triggered by the breakdown of hydrous minerals within the partially removed mantle lithosphere. This Nb signature is most apparent in the Plio-Pleistocene phase of volcanism of the eastern Intersalar Range of the central Altiplano, particularly in the lavas of Coracora volcano, although also recognizable in the Miocene samples.

The remaining mantle lithospheric root beneath the central Altiplano suggests that the process of piecemeal foundering is either ongoing, and/or represents a potential location of future lithospheric foundering. High ³He/⁴He values of geothermal spring water near Coracora volcano in the eastern Intersalar Range, as well as in the broader region, indicate that mantle melting and storage beneath the Altiplano is either recent (<< 1 Ma) or active (Hoke and Lamb, 2007), suggesting an ongoing melting trigger beneath the plateau.

Although alternative explanations can be invoked, relatively low ⁸⁷Sr/⁸⁶Sr values hint at a contribution of isotopically depleted mantle lithosphere (e.g., Rogers and Hawkesworth, 1989) and share similarities with alkaline magmatism related to lithospheric foundering in the southern Puna and northern Altiplano reararc regions of the Central Andean Plateau. Pb isotope variations also show correlation with the mantle lithospheric root beneath the central Altiplano, however, variations in crustal Pb compositions may also explain these data. Decompression melting of the asthenosphere and magma mixing, crustal assimilation, and homogenization of magmas in the thick Andean crust all obscure the contributions of the mantle lithosphere in Central Andean lavas. In the absence of mafic magmatism and clear isotopic signatures, Nb systematics may provide important clues of the mantle source components.

Data availability statement

The original contributions presented in the study are included in the article/Supplementary Material, further inquiries can be directed to the corresponding author.

Author contributions

MS Principle Investigator. Developed the project in collaboration with NJ and Jon P. Davidson. Wrote the grants for funding, led the field investigations, performed the majority

of sample preparation, coordinated all analytical analyses, interpreted the results, primary author of manuscript. NJ Collaborated with the overall development of the project. Coordinated field excursions. Participated in discussions regarding results and interpretations and contributed input and text for the manuscript. DB led the investigations of the ⁴⁰Ar/³⁹Ar age data. Wrote sections of the manuscript regarding the Ar-Ar data. Reviewed manuscript and contributed to interpretations and conclusions of the study.

Funding

This research was performed by MS as part of the International Junior Research Fellowship program at Durham University. The Department of Earth Sciences at Durham University provided additional funding for fieldwork, thin section preparation, and isotope analyses. Funding for ⁴⁰Ar/³⁹Ar age determinations was provided by the Natural Environmental Research Council (NERC). The Instituto de Investigaciones Geológicas y del Medio Ambiente at the Universidad Mayor de San Andrés provided vehicles for fieldwork.

Acknowledgments

We are extremely grateful for the mentorship of Jon P. Davidson at Durham University, whose lifetime of work in the Central Andes laid the foundation for this study. We also thank three anonymous reviewers for their helpful comments which greatly improved this manuscript.

Conflict of interest

The authors declare that the research was conducted in the absence of any commercial or financial relationships that could be construed as a potential conflict of interest.

Publisher's note

All claims expressed in this article are solely those of the authors and do not necessarily represent those of their affiliated organizations, or those of the publisher, the editors and the reviewers. Any product that may be evaluated in this article, or claim that may be made by its manufacturer, is not guaranteed or endorsed by the publisher.

Supplementary material

The Supplementary Material for this article can be found online at: <https://www.frontiersin.org/articles/10.3389/feart.2022.917488/full#supplementary-material>

References

- Aitchison, S. J., Harmon, R. S., Moorbath, S., Schneider, A., Soler, P., Soria-Escalante, E., et al. (1995). Pb isotopes define basement domains of the Altiplano, central Andes. *Geol.* 23 (6), 555–558. doi:10.1130/0091-7613(1995)023<0555:pidbdo>2.3.co;2
- Allmendinger, R. W., Jordan, T. E., Kay, S. M., and Isacks, B. L. (1997). The evolution of the Altiplano-Puna Plateau of the central Andes. *Annu. Rev. Earth Planet. Sci.* 25, 139–174. doi:10.1146/annurev.earth.25.1.139
- Allmendinger, R. W., Smalley, R., Jr., Bevis, M., Caprio, H., and Brooks, B. (2005). Bending the Bolivian orocline in real time. *Geol.* 33 (11), 905–908. doi:10.1130/g21779.1
- Almendras, O. (2002). Rio mulato quadrangle, SE 19-16: Thematic maps of mineral resources of Bolivia, publication SGB serie II-MTB-10B, GEOBOL-SGAB, scale 1:250,000, 1 sheet.
- Baker, M., and Francis, P. (1978). Upper cenozoic volcanism in the central Andes – ages and volumes. *Earth Planet. Sci. Lett.* 41, 175–187. doi:10.1016/0012-821X(78)90008-0
- Barnes, J. B., and Ehlers, T. A. (2009). End member models for Andean Plateau uplift. *Earth-Science Rev.* 97, 105–132. doi:10.1016/j.earscirev.2009.08.003
- Beck, S. L., and Zandt, G. (2002). The nature of orogenic crust in the central Andes. *J. Geophys. Res.* 107, ESE 7-1–ESE 7-16. doi:10.1029/2000JB000124
- Blum-Oeste, M., and Wörner, G. (2016). Central Andean magmatism can be constrained by three ubiquitous endmembers. *Terra nova.* 28, 434–440. No. 6. doi:10.1111/ter.12237
- Cahill, T., and Isacks, B. L. (1992). Seismicity and shape of the subducted Nazca plate. *J. Geophys. Res.* 97, 17503529. . B12503–17. doi:10.1029/92JB00493
- Carlier, G., Lorand, J. P., Liegeois, J. P., Fornari, M., Soler, P., Carlotto, V., et al. (2005). Potassic–ultrapotassic mafic rocks delineate two lithospheric mantle blocks beneath the southern Peruvian Altiplano. *Geol.* 33, 601–604. doi:10.1130/G21643.1
- Correa, N. A. (2011). Evolución Geológica y Petroológica del complejo volcánico Quimsachata – aroma, Región de Tarapacá, Andes Centrales del Norte de Chile. Santiago, Chile: Universidad de Chile, 210. [Ph.D. thesis].
- Davidson, J. P., and de Silva, S. L. (1995). Late cenozoic magmatism of the Bolivian Altiplano. *Contr. Mineral. Pet.* 119, 387–408. doi:10.1007/bf00286937
- Davidson, J. P., and de Silva, S. L. (1992). Volcanic rocks from the Bolivian Altiplano: Insights into crustal structure, contamination, and magma Genesis in the central Andes. *Geol.* 20, 1127–1130. doi:10.1130/0091-7613(1992)020<1127:vrftba>2.3.co;2
- Davidson, J. P., Turner, S., Handley, H., Macpherson, C., and Dosseto, A. (2007). Amphibole “sponge” in the arc crust? *Geol.* 35 (9), 787–790. doi:10.1130/G23637a.1
- de Silva, S., Davidson, J. P., Croudace, I. W., and Escobar, A. (1993). Volcanological and petrological evolution of volcan Tata Sabaya, SW Bolivia. *J. Volcanol. Geotherm. Res.* 55, 305–335. doi:10.1016/0377-0273(93)90043-q
- DeCelles, P. G., Zandt, G., Beck, C. A., Currie, C. A., Ducea, M. N., Kapp, P., et al. (2015). “Cyclical orogenic processes in the cenozoic central Andes,” in *Geodynamics of a cordilleran orogenic system: The central Andes of Argentina and northern Chile*. Editors P. G. DeCelles, M. N. Ducea, B. Carrapa, and P. A. Kapp (USA: Geological Society of America Memoir), 212, 459–490. doi:10.1130/2015.1212(22)
- Deino, A. L. (2015). Berkeley geochronology center, mass spec, 40Ar/39Ar data measurement and reduction software. Available at: http://www.bgc.org/facilities/other_facil.html.
- Drew, S. T., Ducea, M. N., and Schoenbohm, M. L. (2009). Mafic volcanism on the Puna Plateau, NW Argentina: Implications for lithospheric composition and evolution with an emphasis on lithospheric foundering. *Lithosphere* 1 (5), 305–318. doi:10.1130/L54.1
- Elger, K., Oncken, O., and Glodny, J. (2005). Plateau-style accumulation of deformation: Southern Altiplano. *Tectonics* 24, TC4020. doi:10.1029/2004TC001675
- Elkins-Tanton, L. T. (2005). “Continental magmatism caused by lithospheric delamination,” in *Plates, plumes, and paradigms*. Editors G. R. Foulger, J. H. Natland, D. C. Presnall, and D. L. Anderson (USA: Geological Society of America Special Paper), 388, 449–461.
- Evernden, J., Kriz, S., and Cherroni, C. (1977). Potassium-Argon ages of some Bolivian rocks. *Econ. Geol.* 72, 1042–1061. doi:10.2113/gsecongeo.72.6.1042
- Feeley, T. C., and Davidson, J. P. (1994). Petrology of Calc-Alkaline Lavas at Volc n Ollag e and the Origin of Compositional Diversity at Central Andean Stratovolcanoes. *J. Petrology* 35, 1295–1340. doi:10.1093/petrology/35.5.1295
- Gardeweg, M., and Sellés, D. (2017). “Characterization of the last volcanic products erupted in the Pica Gap (Northern Chile),” in *Actas XX congreso geológico argentino* (Sesión Técnica: Universidad de Chile), 7, 60–67.
- GeoROC Database. ANDEAN_ARC.csv, 2012, Available at: <http://georoc.mpch-mainz.gwdg.de/georoc>.
- Grant, J., Halls, C., Salinas, W., and Snelling, N. (1979). K-Ar ages of igneous rocks and mineralization in part of the Bolivian Tin Belt. *Econ. Geol.* 74, 838–851. doi:10.2113/gsecongeo.74.4.838
- Handley, H. K., Macpherson, C. G., Davidson, J. P., Berlo, K., and Lowry, D. (2007). Constraining fluid and sediment contributions to subduction-related magmatism in Indonesia: Ijen volcanic complex. *J. Petrology* 48, 1155–1183. doi:10.1093/petrology/egm013
- Hildreth, W., and Moorbath, S. (1988). Crustal contributions to arc magmatism in the Andes of central Chile. *Contr. Mineral. Pet.* 98, 455–489. doi:10.1007/BF00372365
- Hoke, L., and Lamb, S. (2007). Cenozoic behind-arc volcanism in the Bolivian Andes, South America: Implications for mantle melt generation and lithospheric structure. *J. Geol. Soc. Lond.* 164, 795–814. doi:10.1144/0016-76492006-092
- Hora, J. M., Singer, B. S., Wörner, G., Beard, B. L., Jicha, B. R., and Johnson, C. M. (2009). Shallow and deep crustal control on differentiation of calc-alkaline and tholeiitic magma. *Earth Planet. Sci. Lett.* 285, 75–86. doi:10.1016/j.epsl.2009.05.042
- Husson, L., and Sempere, T. (2003). Thickening the Altiplano crust by gravity-driven crustal channel flow. *Geophys. Res. Lett.* 30. doi:10.1029/2002GL016877
- Ionov, D. A., Griffin, W. L., and O'Reilly, S. Y. (1997). Volatile-bearing minerals and lithophile trace elements in the upper mantle. *Chem. Geol.* 141, 153–184. doi:10.1016/S0009-2541(97)00061-2
- Irvine, T. N., and Baragar, W. R. A. (1971). A guide to the chemical classification of the common volcanic rocks. *Can. J. Earth Sci.* 8 (5), 523–548. doi:10.1139/e71-055
- James, D. E., and Sacks, I. S. (1999). “Cenozoic formation of the central Andes: A geophysical perspective,” in *Geology and ore deposits of the central Andes*. Editor B. J. Skinner (Tulsa, Oklahoma: SEPM Special Publication), 1–25.
- Jiménez, N., and López-Velásquez, S. (2008). Magmatism in the Huarina belt, Bolivia, and its geotectonic implications. *Tectonophysics* 459, 85–106. doi:10.1016/j.tecto.2007.10.012
- Johnson, D. M., Hooper, P. R., and Conrey, R. M. (1999). XRF analysis of rocks and minerals for major and trace elements on a single low-dilution Li-tetraborate fused bead. *Adv. X-Ray Analysis* 41, 117–132.
- Kato, J. J. (2013). *Geochemistry of the neogene Los Frailes ignimbrite complex of the central andean Altiplano plateau* [Ph.D. Thesis. Ithaca, New York: Cornell University, 173.
- Kay, R. M., and Kay, S. M. (1993). Delamination and delamination magmatism. *Tectonophysics* 219 (13), 177–189. doi:10.1016/0040-1951(93)90295-u
- Kay, S. M., Coira, B. L., Caffè, P. J., and Chen, C. (2010). Regional chemical diversity, crustal and mantle sources and evolution of central Andean Puna plateau ignimbrites. *J. Volcanol. Geotherm. Res.* 198, 81–111. doi:10.1016/j.jvolgeores.2010.08.013
- Kay, S. M., Coira, B., and Viramonte, J. (1994). Young mafic back arc volcanic rocks as indicators of continental lithospheric delamination beneath the Argentine Puna Plateau, central Andes. *J. Geophys. Res.* 99, 24323–24339. doi:10.1029/94JB00896
- Kennen, L., Lamb, S., and Rundle, C. (1995). K-Ar dates from the Altiplano and Cordillera oriental of Bolivia: Implications for cenozoic stratigraphy and tectonics. *J. South Am. Earth Sci.* 8, 163–186. doi:10.1016/0895-9811(95)00003-x
- Knaack, C., Cornelius, S. B., and Hooper, P. R. (1994). *Technical notes: Trace element analyses of rocks and minerals by ICP-ms: Pullman*. Washington: GeoAnalytical Laboratory, Washington State University Open-File Report.
- Le Maitre, R. W., Bateman, P., Dudek, A., Keller, J., Lameyre Le Bas, M. J., Sabine, et al. (1989). *A classification of igneous rocks and glossary of terms*. Oxford: Blackwell, 193.
- Leytón, F., and Jurado, E. (1995). Salinas de Garci Mendoza quadrangle, SE 19-15: Thematic maps of mineral resources of Bolivia, publication SGB serie II-MTB-4B, GEOBOL-SGAB, scale 1:250,000, 1 sheet.
- Lindsay, J. M., Schmitt, A. K., Trumbull, R. B., de Silva, S. L., Siebel, W., and Emmermann, R. (2001). Magmatic evolution of the La Pacana caldera system, Central Andes, Chile: Compositional variation of two cogenetic, large-volume felsic ignimbrites. *J. Petrology* 42 (3), 459–486. doi:10.1093/petrology/42.3.459
- Lucassen, F., Franz, G., Romer, R. L., Schultz, F., Dulski, P., and Wemmer, K. (2007). Pre-Cenozoic intra-plate magmatism along the Central Andes (17–34S): Composition of the mantle at an active margin. *Lithos* 99, 312–338. doi:10.1016/j.lithos.2007.06.007
- Lucassen, F., Franz, G., Viramonte, J., Romer, R. L., Dulski, P., and Lang, A. (2005). The late Cretaceous lithospheric mantle beneath the Central Andes:

- Evidence from phase equilibria and composition of mantle xenoliths. *Lithos* 82, 379–406. doi:10.1016/j.lithos.2004.08.002
- Mamani, M., Wörner, G., and Semper, T. (2010). *Geochemical variations in igneous rocks of the central Andean orocline (13°S to 18°S): Tracing crustal thickening and magma generation through time and space*, 122. USA: Geological Society of America Bulletin, 162–182. doi:10.1130/B26538.1
- Mark, D., Barfod, D., Stuart, F., and Imlach, J. (2009). The ARGUS multicollector noble gas mass spectrometer: Performance for $^{40}\text{Ar}/^{39}\text{Ar}$ geochronology. *Geochem. Geophys. Geosyst.* 10, Q0AA02. doi:10.1029/2009gc002643
- Maro, G., Caffè, P. J., Romer, R. L., and Trumbull, R. B. (2017). Neogene mafic magmatism in the northern Puna Plateau, Argentina: Generation and evolution of a back-arc volcanic suite. *J. Petrology* 58 (8), 1591–1617. doi:10.1093/ptrology/egx066
- McGlashan, N., Brown, L., and Kay, S. (2008). Crustal thickness in the central Andes from teleseismically recorded depth phase precursors. *Geophys. J. Int.* 175 (3), 1013–1022. doi:10.1111/j.1365-246X.2008.03897.x
- McLeod, C. L., Davidson, J. P., Nowell, G. M., and de Silva, S. L. (2012). Disequilibrium melting during crustal anatexis and implications for modeling open magmatic systems. *Geology* 40, 435–438. doi:10.1130/G33000.1
- McLeod, C. L., Davidson, J. P., Nowell, G. M., de Silva, S. L., and Schmitt, A. K. (2013). Characterizing the continental basement of the Central Andes: Constraints from Bolivian crustal xenoliths. *Geol. Soc. Am. Bull.* 125 (5–6), 985–997. doi:10.1130/B30721.1
- McQuarrie, N., Horton, B. K., Zandt, G., Beck, S., and DeCelles, P. G. (2005). Lithospheric evolution of the Andean fold-thrust belt, Bolivia, and the origin of the central Andean Plateau. *Tectonophysics* 399, 15–37. doi:10.1016/j.tecto.2004.12.013
- Murray, K. E., Ducea, M. N., and Schoenbohm, L. (2015). “Foundering-driven lithospheric melting: The source of central Andean mafic lavas on the Puna Plateau (22°S–27°S),” in *Geodynamics of a cordilleran orogenic system: The central Andes of Argentina and northern Chile*. Editors P. G. DeCelles, M. N. Ducea, B. Carrapa, and P. A. Kapp (USA: Geological Society of America Memoir), 212, 139–166. doi:10.1130/2015.1212(08)
- Niespolo, E. M., Rutte, D., Deino, A. L., and Renne, P. R. (2017). Intercalibration and age of the Alder Creek sanidine $^{40}\text{Ar}/^{39}\text{Ar}$ standard. *Quat. Geochronol.* 39, 205–213. doi:10.1016/j.quageo.2016.09.004
- Oncken, O., Hindle, D., Kley, J., Elger, K., Victor, P., and Schemmann, K. (2006). “Deformation of the central andean upper plate system — Facts, fiction, and constraints for plateau models,” in *The Andes: Active subduction orogeny*. Editors O. Oncken, G. Chong, G. Franz, P. Giese, H.-J. Gotze, V. A. Ramos, et al. (Berlin: Springer-Verlag), 3–27.
- Peccerillo, A., and Taylor, S. R. (1976). Geochemistry of Eocene calc-alkaline volcanic rocks from the Kastamonu area, Northern Turkey. *Contr. Mineral. Pet.* 58, 63–81. doi:10.1007/BF00384745
- Pilet, S., Baker, M. B., and Stolper, E. M. (2008). Metasomatized lithosphere and the origin of alkaline lavas. *Science* 320, 916–919. N. 5878no. 5878. doi:10.1126/science.1156563
- Polanco, E., and Gardeweg, M. (2000). “Antecedentes Preliminares de la Estratigrafía volcánica del Cenozoico Superior en los Cuadrangulos Pampa Lirima y Cancosa, Altiplano de la I Región,” in *Chile (19°45′–20°00′S Y 69°00′–68°30′W), congreso geológico chileno*, 9 (Puerto Varas, Chile, 324–328. 31 Julio – 4 Agosto.
- Risse, A., Trumbull, R. B., Kay, S. M., Coira, B., and Romer, R. L. (2013). Multi-stage evolution of late neogene mantle-derived magmas from the central Andes back-arc in the southern Puna Plateau of Argentina. *J. Petrology* 54 (10), 1963–1995. doi:10.1093/ptrology/egt038
- Rogers, G. R., and Hawkesworth, C. J. (1989). A geochemical traverse across the north Chilean Andes: Evidence for crust generation from the mantle wedge. *Earth Planet. Sci. Lett.* 91, 271–285. doi:10.1016/0012-821X(89)90003-4
- Rollinson, H. R. (1993). *Using geochemical data: Evaluation, presentation, interpretation*. Essex: Longman, 102–170.
- Salisbury, M. J., Jicha, B. R., de Silva, S. L., Singer, B. S., Jiménez, N. C., and Ort, M. H. (2011). $^{40}\text{Ar}/^{39}\text{Ar}$ chronostratigraphy of Altiplano-Puna volcanic complex ignimbrites reveals the development of a major magmatic province. *Geol. Soc. Am. Bull.* 123, 821–840. 5–6. doi:10.1130/B30280.1
- Salisbury, M. J., Kent, A. J. R., Jiménez, N., and Jicha, B. R. (2015). Geochemistry and $^{40}\text{Ar}/^{39}\text{Ar}$ geochronology of lavas from Tunupa volcano, Bolivia: Implications for plateau volcanism in the central Andean Plateau. *Lithosphere* 7 (2), 95–107. doi:10.1130/L399.1
- Schultz, F., Lehmann, B., Tawackoli, S., Rössling, R., Belyatsky, B., and Dulski, P. (2004). Carbonatite diversity in the central Andes: The Ayopaya alkaline province, Bolivia. *Contrib. Mineral. Pet.* 148, 391–408. doi:10.1007/s00410-004-0612-0
- Sellés, D., Gardeweg, M., and Gartibaldi, N. (2016). *Geología de Área Pampa Lirima-cancosa, región de Tarapacá, servicio nacional de Geología y minería (SERNAGEOMIN), serie geología básica, No. 182. 1 sheet, 1:100,000 scale*. Santiago, Chile. doi:10.13140/RG.2.2.35023.18086
- Sparks, R. S. J., Folkes, C. B., Humphreys, M. C. S., Barfod, D. N., Clavero, J., Sunagua, M. C., et al. (2008). Uturuncu volcano, Bolivia: Volcanic unrest due to mid-crustal magma intrusion. *Am. J. Sci.* 308 (6), 727–769. doi:10.2475/06.2008.01
- Sun, S., and McDonough, W. F. (1989). “Chemical and isotopic composition of oceanic basalts: Implications for mantle compositions and processes,” in *Magmatism in the ocean basins*. Editors A. D. Saunders and M. J. Norry (London: Geological Society of London Special Publication), 42, 313–345.
- Trumbull, R. B., Ulrich, R., Oncken, O., Ekkehard, S., Munier, K., and Hongn, F. (2006). “The time-space distribution of cenozoic volcanism in the south-central Andes: A new data compilation and some tectonic implications,” in *The Andes: Active subduction orogeny*. Editors O. Oncken, G. Chong, G. Franz, P. Giese, H.-J. Gotze, V. A. Ramos, et al. (Berlin: Springer-Verlag), 29–43.
- Victor, P., Oncken, O., and Glodny, J. (2004). Uplift of the Western Altiplano plateau: Evidence from the Precordillera between 20 and 21°S (northern Chile). *Tectonics* 23, TC4004. doi:10.1029/2003TC001519
- Walker, B. A. (2011). “The geochemical evolution of the Aucanquilcha volcanic cluster: Prolonged magmatism and its crustal consequences,” (Corvallis, Oregon: Oregon State University), 199. [Ph.D. thesis].
- Wendt, I., and Carl, C. (1991). The statistical distribution of the mean squared weighted deviation. *Chem. Geol. Isot. Geosci. Sect.* 86, 275–285. doi:10.1016/0168-9622(91)90010-t
- Wörner, G., Moorbath, S., and Harmon, R. S. (1992). Andean Cenozoic volcanic centers reflect basement isotopic domains. *Geol.* 20, 1103–1106. doi:10.1130/0091-7613(1992)020<1103:acvcr>2.3.co;2
- Wörner, G., Moorbath, S., Horn, S., Entenmann, J., Harmon, R. S., Davidson, J. P., et al. (1994). “Large geochemical variations along the Andean arc of northern Chile (17.5–22°S),” in *Tectonics of the southern central Andes: Structure and evolution of an active continental margin*. Editors K. J. Reutter, E. Scheuber, and P. J. Wigger (Berlin: Springer-Verlag), 77–91.
- Yuan, X., Sobolev, S. V., and Kind, R. (2002). Moho topography in the central Andes and its geodynamic implications. *Earth Planet. Sci. Lett.* 199, 389–402. doi:10.1016/S0012-821X(02)00589-7